



# Visual Scanning Hartmann Optical Tester (VSHOT) Uncertainty Analysis

A. Gray, A. Lewandowski, and T. Wendelin  
*National Renewable Energy Laboratory*

**NREL is a national laboratory of the U.S. Department of Energy, Office of Energy Efficiency & Renewable Energy, operated by the Alliance for Sustainable Energy, LLC.**

**Milestone Report**  
NREL/TP-5500-48482  
October 2010

Contract No. DE-AC36-08GO28308

# Visual Scanning Hartmann Optical Tester (VSHOT) Uncertainty Analysis

A. Gray, A. Lewandowski, and T. Wendelin  
*National Renewable Energy Laboratory*

Prepared under Task No. CP09.1001

NREL is a national laboratory of the U.S. Department of Energy, Office of Energy Efficiency & Renewable Energy, operated by the Alliance for Sustainable Energy, LLC.

## NOTICE

This report was prepared as an account of work sponsored by an agency of the United States government. Neither the United States government nor any agency thereof, nor any of their employees, makes any warranty, express or implied, or assumes any legal liability or responsibility for the accuracy, completeness, or usefulness of any information, apparatus, product, or process disclosed, or represents that its use would not infringe privately owned rights. Reference herein to any specific commercial product, process, or service by trade name, trademark, manufacturer, or otherwise does not necessarily constitute or imply its endorsement, recommendation, or favoring by the United States government or any agency thereof. The views and opinions of authors expressed herein do not necessarily state or reflect those of the United States government or any agency thereof.

Available electronically at <http://www.osti.gov/bridge>

Available for a processing fee to U.S. Department of Energy and its contractors, in paper, from:

U.S. Department of Energy  
Office of Scientific and Technical Information

P.O. Box 62  
Oak Ridge, TN 37831-0062  
phone: 865.576.8401  
fax: 865.576.5728  
email: <mailto:reports@adonis.osti.gov>

Available for sale to the public, in paper, from:

U.S. Department of Commerce  
National Technical Information Service  
5285 Port Royal Road  
Springfield, VA 22161  
phone: 800.553.6847  
fax: 703.605.6900  
email: [orders@ntis.fedworld.gov](mailto:orders@ntis.fedworld.gov)  
online ordering: <http://www.ntis.gov/help/ordermethods.aspx>

Cover Photos: (left to right) PIX 16416, PIX 17423, PIX 16560, PIX 17613, PIX 17436, PIX 17721



Printed on paper containing at least 50% wastepaper, including 10% post consumer waste.

# Table of Contents

|                                                                 |    |
|-----------------------------------------------------------------|----|
| Table of Contents .....                                         | 1  |
| Abstract .....                                                  | 2  |
| Introduction .....                                              | 3  |
| VSHOT .....                                                     | 3  |
| Zernike Polynomial .....                                        | 5  |
| Uncertainty Contributions .....                                 | 9  |
| Target Tilt .....                                               | 12 |
| Target Face to Laser Scanner Output.....                        | 13 |
| Instrument Vertical Offset .....                                | 14 |
| Scanner Tilt.....                                               | 16 |
| Distance from Target to Test Piece .....                        | 18 |
| Camera Calibration.....                                         | 20 |
| Scanner/Calibration .....                                       | 25 |
| Uncertainty Estimate – Slope Error .....                        | 29 |
| Uncertainty Estimate – Focal Length and Test Article Tilt ..... | 35 |
| Summary .....                                                   | 36 |
| Acknowledgements.....                                           | 37 |
| References .....                                                | 37 |

## Abstract

Concentrating solar power plants are being developed and deployed around the world using various concentrator technologies, including parabolic troughs, power towers, and dishes. Sunlight is focused onto a receiver that collects the heat to generate steam for a conventional power plant or Stirling engine. To concentrate sunlight and achieve the high temperatures needed to obtain high cycle efficiency, these technologies typically use reflective optics. Glass mirrors are commonly used, but reflective films can also be employed. In either case, the reflective surface needs to concentrate the sunlight by reflecting it to a desired location. This is done by designing the reflective surface to conform to a certain shape that will optimize the amount of light reaching the receiver. Once a reflector has been designed and fabricated, it is important to know how close it is to the ideal shape. The Video Scanning Hartmann Optical Tester (VSHOT) is a surface slope and contour measuring tool for concentrating solar power (CSP) reflector panels used in line- and point-focus technologies. VSHOT was developed by the U.S. Department of Energy's SunLab in the early 1990s in a collaboration between the National Renewable Energy Laboratory (NREL) and Sandia National Laboratories (Sandia) to provide accurate surface characterization of CSP reflective surfaces.

The VSHOT is a proven tool that has been used on heliostat, dish, and trough mirror facets to provide accurate surface slope deviations that characterize optical quality. These data are used to estimate optical performance within the overall system. A study of the uncertainty and sensitivity of this instrument was completed in 1997 showed that there was a 0.1 mrad slope uncertainty in a full scan. Since then, the hardware and software have been upgraded with new technology. To ensure that both industry and laboratory users understand the accuracy of the data provided by the VSHOT, we have conducted a new uncertainty analysis.

This analysis is based primarily on the geometric optics of the system and shows sensitivities to various design and operational parameters. We discuss sources of error with measuring devices, instrument calibrations, and operator measurements for a parabolic trough test. These help to guide the operator in proper setup, and help end users to understand the data they are provided. In this report, we include both the systematic (bias) and random (precision) errors for VSHOT testing and their contributions to the uncertainty. The contributing factors that we considered in this study are the following: target tilt; target face to laser output distance; instrument vertical offset; scanner tilt; distance between the tool and the test piece; camera calibration; and scanner/calibration. These contributing factors were applied to the calculated slope error, focal length, and test article tilt that are generated by the VSHOT data processing. The results shown in this work estimate the  $2\sigma$  slope error uncertainty for a parabolic trough line scan test to be from  $\pm 0.21 - 0.46$  mrad for any given single slope error measurement. The  $2\sigma$  uncertainty for slope errors over a single scan is  $\pm 0.33$  mrad,  $\pm 0.6$  mm ( $\pm 0.03\%$ ) for focal length and  $\pm 0.2$  mrad for test article tilt.

## Introduction

Measurement error is defined as the difference between the true and measured value [1] and includes both the systematic and random errors. The measurement uncertainty discussed in this report provides an estimate of the  $2\sigma$  error in the slope of a reflective surface that may be expected for VSHOT testing. Errors larger than the stated uncertainty will occur 5% of the time.

A previous uncertainty analysis [2] used a 16-inch telescope mirror to conduct the experimental analysis. The distance between the mirror and the VSHOT ranged from 6.32–8.20 m (249–323”). With this setup, the full cone angle for the laser to scan the entire mirror was less than 0.0698 radians ( $4^\circ$ ). The VSHOT is often used to test flat and parabolic trough facets that require the laser to scan a 1.38-radian ( $80^\circ$ ) arc to collect data over the entire test piece. The analysis presented here is for laser scanning angles of  $\pm 0.69$  radians ( $\pm 40^\circ$ ), or 1.38 radians ( $80^\circ$ ). The case study for this uncertainty analysis is an ideal parabolic trough with a 6-m aperture, a 1.71-m focal length, and continuous reflective surface. VSHOT is assumed to have a  $\pm 0.69$  radian cone angle and is 4.928 m (194”) away from the vertex of the collector. This arrangement was selected because it represents a majority of the VSHOT tests conducted.

## VSHOT

The VSHOT is a laser ray-trace system designed to characterize the optical surfaces of solar concentrators [2]. Originally designed to test point-focus (dish) concentrators, it was later modified to include characterization of line-focus (trough) concentrators and has been used to test mirror panels for heliostats. The VSHOT uses computer controlled laser scanner and digital camera to provide surface contour data. The laser scans a mirror in a pattern predefined by the user. At each scanned position, the laser beam is reflected back to a target and the location is imaged using a camera. The surface slope is calculated at each position using the laser output angle and return-spot location. A Zernike Polynomial is used to mathematically fit the surface using the slope data.

During setup and before each test, many of the components are checked and measurements are taken to insure correct orientation of the VSHOT relative to the test article. This procedure is listed below:

1. Level the front of the target.
2. Level the optical rail (Figure 1).
3. Calibrate the camera to the target (Figure 2). Measure the distance between the laser output mirror on the scanner head and the target face.
4. Determine the VSHOT vertical location. Check the level of the target and the scanner again while another operator checks the location of the laser at the vertex of the collector.
5. Measure the distance between the target face and vertex of the trough.
6. Begin a test using the VSHOT software.

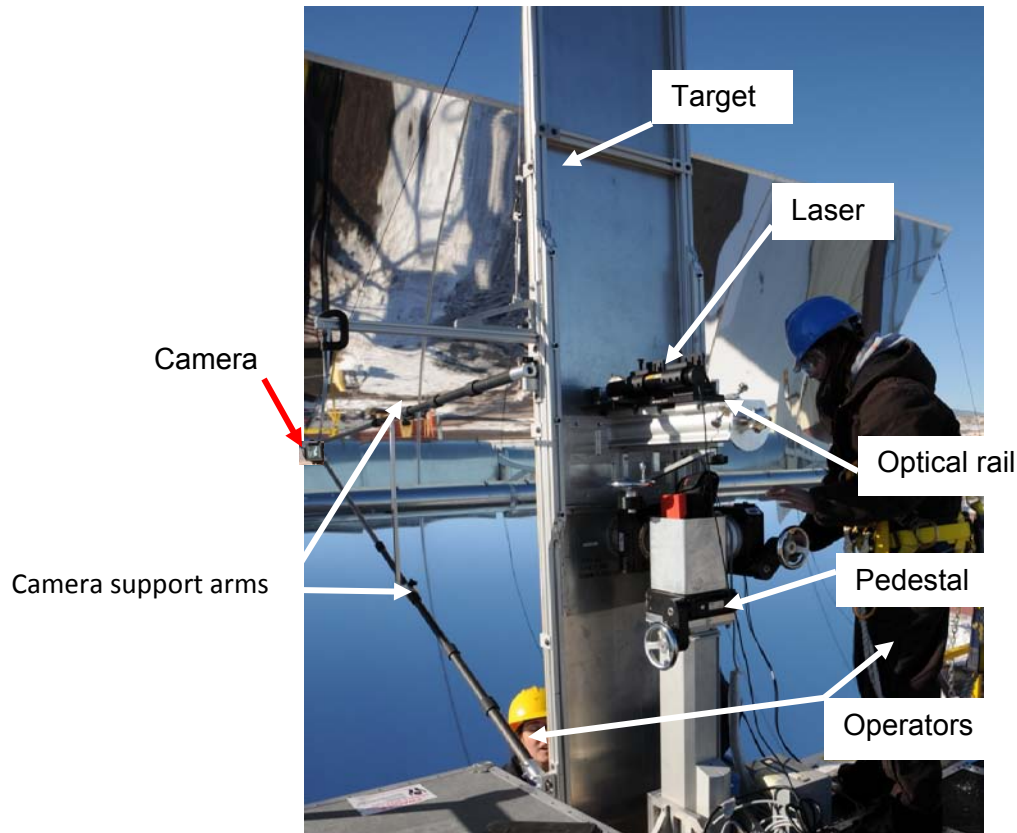


**Figure 1.** Image of the VSHOT TO-GO being set up for a test. The optical rail and target were being leveled at the time this picture was taken. “TO-GO” refers to the version of the hardware used for field testing. (credit: Jen Crawford, NREL)

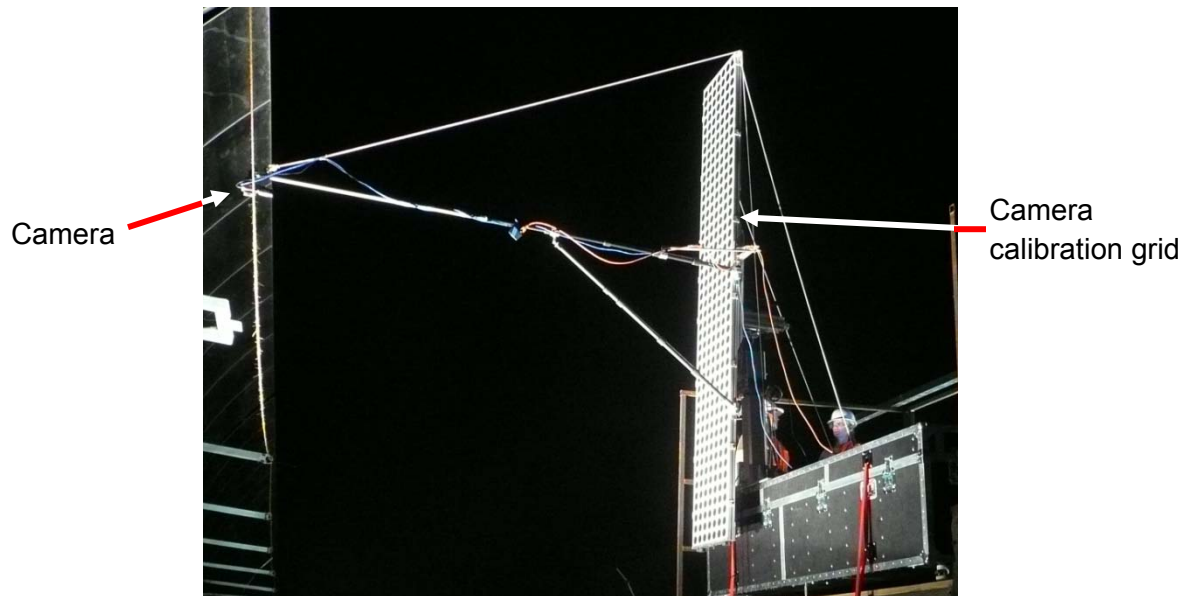


**Figure 2.** Image of the VSHOT “TO-GO” camera calibration grid used to calibrate the camera pixel space to the target. (credit: Mark Bernardi, NREL)

## Zernike Polynomial

A Zernike Polynomial is used to mathematically describe common optical surfaces [3] where  $k$  is the order of the monomial and the  $\Delta x$  and  $\Delta y$  terms compensate for known position offsets of the mirror vertex relative to VSHOT coordinates. These last two terms are useful when fitting the data from an actual test, but for the purpose of this analysis, we will assume they are equal to zero (errors associated with the offset are accounted for in the instrument vertical offset).

$$z(x - \Delta x, y - \Delta y) = \sum_{i=0}^k \sum_{j=0}^i B_{i,j} (x - \Delta x)^j (y - \Delta y)^{i-j} \quad \text{Equation 1}$$

Equation 2 is the second-order expansion where  $k=2$ .

$$z(x, y) = B_{0,0} + B_{1,0}y + B_{1,1}x + B_{2,0}y^2 + B_{2,1}xy + B_{2,2}x^2 \quad \text{Equation 2}$$

Most surfaces tested by VSHOT are parabolic, making the relationship between a second-order Zernike Polynomial equation and the designed surface correlation simple (dish and heliostat mirror panel focal lengths are often long enough such that a sphere and parabola are essentially identical). An ideal parabola can be mathematically described in three dimensions as

$$z(x, y) = \frac{x^2}{4f_x} + \frac{y^2}{4f_y} \quad \text{Equation 3}$$

with coefficient  $f_x$  equal to the focal length in the x direction and  $f_y$  equal to the focal length in the y direction. If we relate Equation 3 to the Zernike monomial,  $B_{2,0} = \frac{1}{4f_y}$  and  $B_{2,2} = \frac{1}{4f_x}$ .  $B_{1,0}$  and  $B_{1,1}$  coefficients describe the test piece tilt relative to the instrument. Under ideal conditions, the tilt terms equal zero. Usually, this is not the case and it is common for these tilt terms to be in the mrad range.

$$\text{tilt}_x = \text{atan}(B_{1,0}) \quad \text{Equation 4}$$

$$\text{tilt}_y = \text{atan}(B_{1,1}) \quad \text{Equation 5}$$

The  $B_{0,0}$  coefficient is the piston term (offset along the z axis).  $B_{2,1}$  is the cross term and is used with the focal length coefficients to determine if there is any astigmatism. If  $B_{2,0} \neq B_{2,2}$  and  $B_{2,1} = 0$ , there is an astigmatism error on the horizontal or vertical axis. If  $B_{2,1} \neq 0$  and  $B_{2,0} \neq B_{2,2}$ , there is an astigmatism error with an arbitrary axis orientation [3]. For a perfect point-focus collector,  $B_{2,0} = B_{2,2} = \frac{1}{4f}$  and  $B_{2,1} = 0$ ; for a perfect line-focus collector  $B_{2,0} = \frac{1}{4f_y}$ ,  $B_{2,2} = 0$ , and  $B_{2,1} = 0$ . Table 1 lists the coefficients for a point-focus and parabola collector.



**Table 1. Zernike coefficients for a perfect point-focus and line-focus collector with a 6-m aperture and 1.71-m focal length and no tilt.**

| Coefficient | Point Focus | Line Focus |
|-------------|-------------|------------|
| $B_{0,0}$   | 0           | 0          |
| $B_{1,0}$   | 0           | 0          |
| $B_{1,1}$   | 0           | 0          |
| $B_{2,0}$   | 0.1462      | 0.1462     |
| $B_{2,1}$   | 0           | 0          |
| $B_{2,2}$   | 0.1462      | 0          |

In this study, a two-dimensional analysis was completed for a parabolic trough collector. Data were generated in a single-column profile because this is representative of the majority of VSHOT field testing. In two dimensions, the Zernike Polynomial can be simplified so that  $z$  is a function of  $y$  only. Assuming a second-order surface ( $k=2$ ), the equation becomes:

$$z(y) = B_0 + B_1y + B_2y^2 \quad \text{Equation 6}$$

with  $B_2 = \frac{1}{4f_y}$  and  $B_1 = \tan(\textit{tilt})$ . For VSHOT testing of troughs in the field, only the slope errors in the transverse,  $y$ , direction (along the curvature) are typically collected (depicted in Figure 3). The laser is scanned in a vertical direction (with the trough facing the horizon, i.e., with a vertical aperture). VSHOT records the output angle of the laser,  $\alpha_y$ , and the return-spot location on the target,  $H_y$ , then uses this information to calculate the slope. The ideal return-spot location is compared to the actual to calculate slope error.

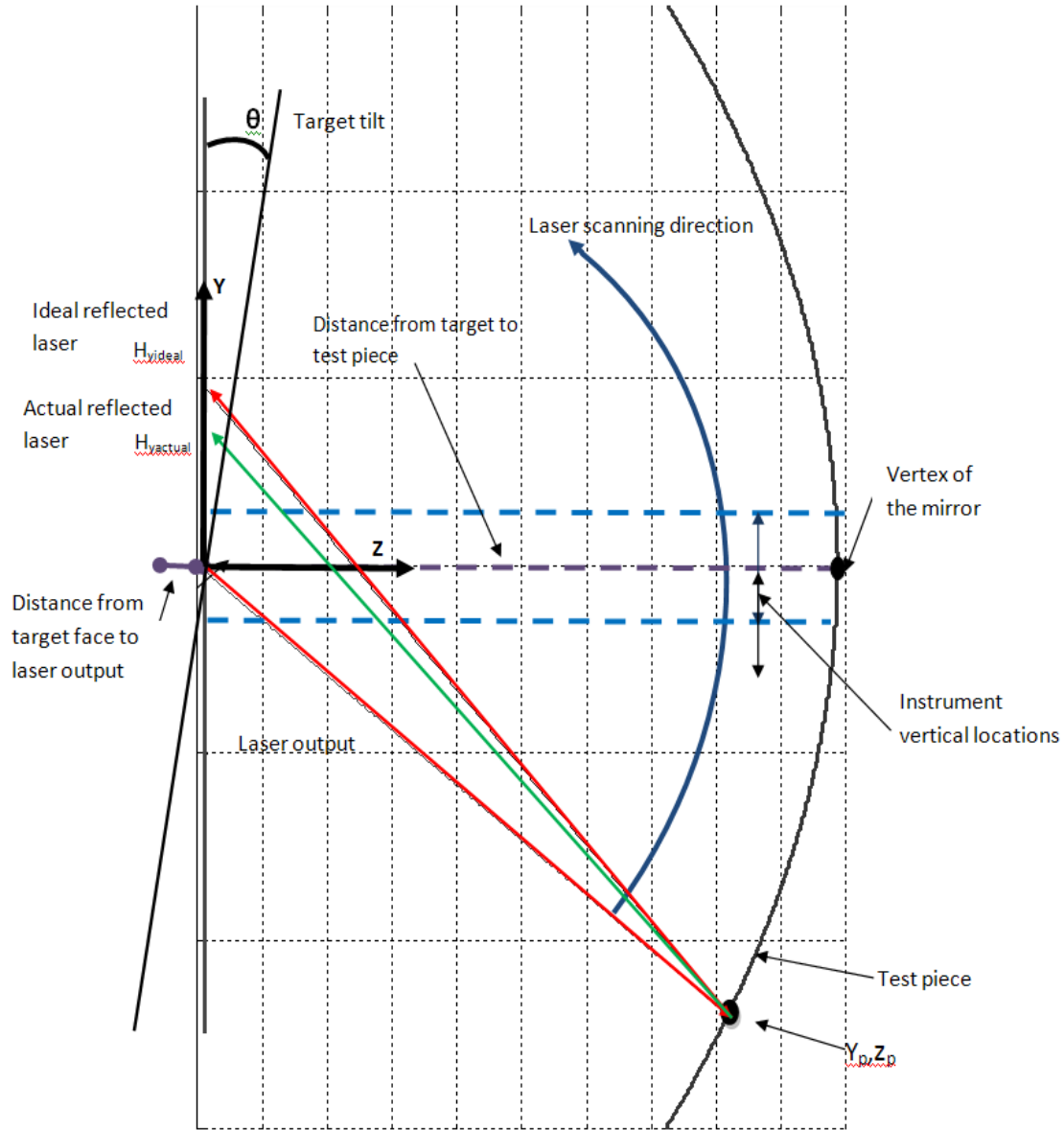


**Figure 3. Schematic of VSHOT used with a trough collector. VSHOT target and laser are on the left and a two-dimensional representation of a parabolic collector is on the right. The red line is the ideal laser output angle as it scans the test piece with its ideal reflection onto the target. The green line is actual simulated reflection caused by the surface slope error at that point on the parabola. This figure is for a 6-m aperture with a 1.71-m focal length, laser output angle of  $-0.531$  radian ( $30.45^\circ$ ). The distance from the target to the vertex of the collector is 4.93 m. The laser hits the collector at  $y_p = -2.40$  m,  $z_p = 5.77$  m. Ideally, the laser return spot on the target is  $H_{y_{ideal}} = 0.948$  m and the actual return spot for this example is  $H_{y_{actual}} = 0.75$  m. With no other setup errors, the slope error at this point is  $+15$  mrad.**

VSHOT results are presented as a slope error,  $R_y$ , for each data point collected, and as an overall root-mean-square (RMS) of the slope errors for either a single scan or test. The RMS slope error is also defined as the sample standard deviation,  $\sigma_{RMS}$  (Equation 7) for a distribution with zero

mean. The slope errors can be provided relative to a best-fit focal length and/or the design focal length.

$$\sigma_{RMS} = \sqrt{\frac{\sum_{i=1}^N R_{y,i}^2}{N-1}} \quad \text{Equation 7}$$

The slope at each point on the test piece is the slope of the tangent line at that point. For the perfect parabolic case, the slope should be linear across the entire surface and can be described mathematically by Equation 8. The effect of focal length on slope is shown in Figure 4.

$$\frac{dz}{dy} = \frac{y}{2f_y} \quad \text{Equation 8}$$

The derivative of the two-dimensional Zernike Polynomial is shown in Equation 9. If there is a tilt in the test piece,  $B_1$  will not be equal to zero and the line will translate in the vertical direction by the value  $B_1$ . An example of this is shown in Figure 5. The slope of the line gives the “best fit” focal length through the  $B_2$  term.  $B_1$  and  $B_2$  are independent and thus can be uniquely determined for a test that provides slope (and slope error) as a function of position along the aperture.

$$\frac{dz}{dy} = B_1 + 2B_2y \quad \text{Equation 9}$$

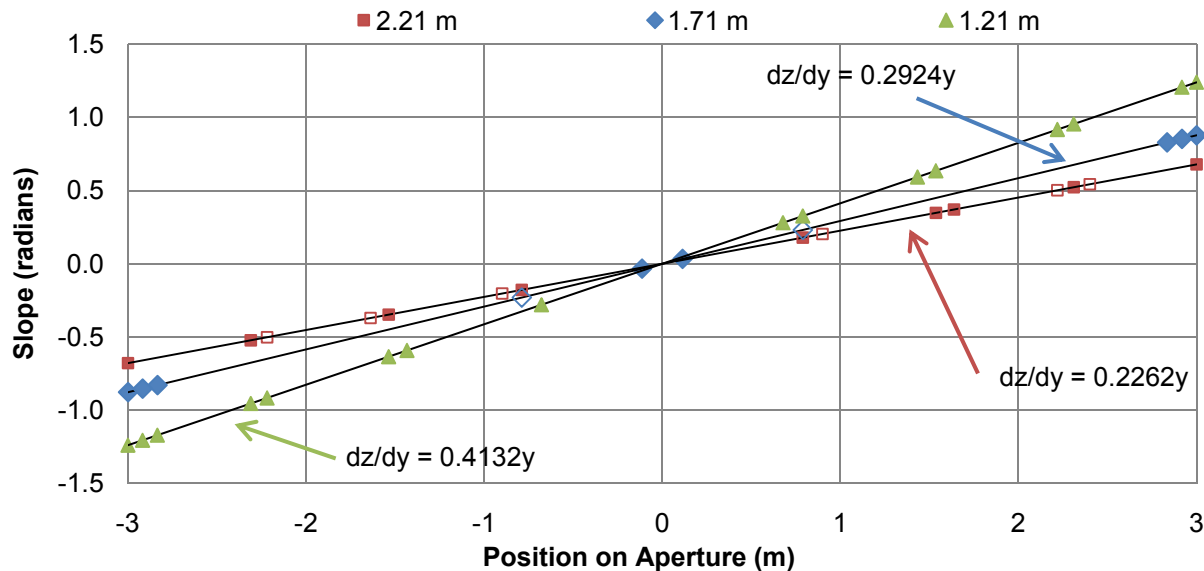


**Figure 4.** This figure shows how the focal length affects the slope,  $dz/dy$ , along the aperture. The surface slope along a parabola with three different focal lengths is plotted, 2.21 m, 1.71 m, and 1.21 m. As the focal length decreases, the slope increases.

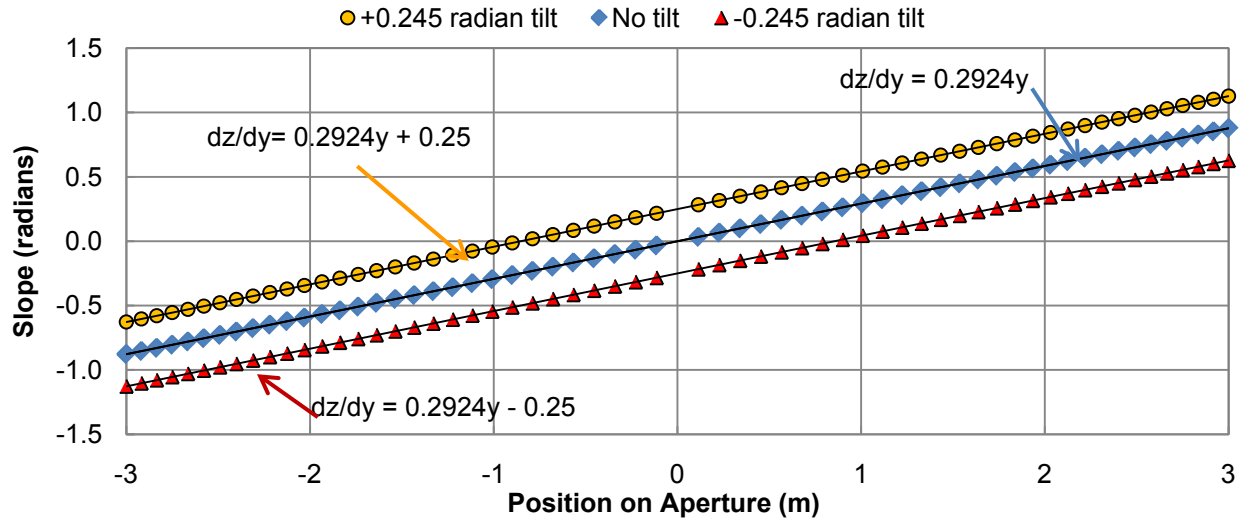


**Figure 5.** This figure shows how tilt affects the slope along the aperture. Tilt does not affect the calculated focal length.

### Uncertainty Contributions

The measurement uncertainty in this paper is applied to the calculated value of the reflective surface slope, focal length, and test-article tilt. The slope (or slope error) is of primary interest, so we primarily address the impacts of measurement error on it and then summarize the impacts on focal length and test-article tilt in a later section. We consider six random error sources and seven systematic error sources in this uncertainty analysis which are listed in Table 2. Random error uncertainty comes from hardware vendor data on repeatability or precision where we have not explicitly distinguished between those two terms. All but the camera calibration random errors will vary over the short time while measurements are being taken. Systematic uncertainty can be difficult to quantify and our assumption is that over a large number of tests the biases imposed by the operator in measuring setup parameters will be randomly distributed. We determined those values based on experience, judgment or some approach specific to each uncertainty. Initially, we show the impact of all the errors considered (except camera calibration and scanner/calibration), then address the individual errors in separate subsections.

The affect on the uncertainty in the calculated slope varies at different laser output angles for each of the uncertainties listed in Table 2. A computer program was written to simulate the test geometry and calculate the impact of the uncertainties listed in Table 2. Figure 6 (random uncertainty) and Figure 7 (systematic uncertainty) show the slope error results for each of the uncertainties listed in Table 2 as a function of laser output angle;  $-0.69$  radians corresponds to  $-40^\circ$  (lower edge of the aperture).

The target tilt is measured with a level that has precision of  $\pm 0.208$  mrad. It is assumed that the operator will cause a systematic error when taking this measurement of  $0.416$  mrad (twice the random error). The target face to laser output is measured with calipers that have an accuracy of  $0.0127$  mm. We estimate the operator can measure this to within  $0.508$  mm of the true value. Overall, these two measurements cause the smallest slope error uncertainties, with less than

0.035 mrad over the aperture. The minimum for both of these contributors is at a laser output angle of 0 radians (vertex of the collector).

**Table 2. List of uncertainties considered in this study. All of the random and systematic errors are assumed to have a 95% confidence ( $2\sigma$ ).**

| Description                         | Measuring Device                                     | Random                                                 | Systematic                              |
|-------------------------------------|------------------------------------------------------|--------------------------------------------------------|-----------------------------------------|
| Target tilt                         | Bubble level                                         | $\pm 0.208$ mrad ( $0.012^\circ$ )                     | $\pm 0.416$ mrad ( $0.024^\circ$ )      |
| Target face to laser scanner output | Calipers                                             | $\pm 0.0127$ mm ( $0.0005''$ )                         | $\pm 0.5$ mm ( $0.02''$ )               |
| Instrument vertical offset          | Human eye                                            | N/A                                                    | $\pm 1.59$ mm ( $0.0625''$ , $1/16''$ ) |
| Scanner tilt                        | Inclinometer                                         | $\pm 0.087$ mrad ( $0.005^\circ$ )                     | $\pm 0.523$ mrad ( $0.03^\circ$ )       |
| Distance from target to test piece  | Laser range finder                                   | $\pm 1.27$ mm ( $0.05''$ )                             | $\pm 0.751$ mm ( $0.030''$ )            |
| Camera calibration                  | Prosilica GE2040 GigE Camera<br>Cambridge Technology | $1.49 \pm 0.084$ mm/pixel<br>( $0.0587 \pm 0.0034''$ ) | $\pm 0.374$ mm/pixel ( $0.014''$ )      |
| Scanner/calibration                 | closed-loop galvanometer model 6220                  | $\pm 8$ $\mu$ rad                                      | $\pm 0.62$ mrad ( $0.36^\circ$ )        |

\* A Visual description for some of these measurements is shown in Figure 3.

The laser, at 0 radians, should be in line with the vertex of the collector as shown in Figure 3. The location of the laser is verified by visually inspecting the location of the laser on the collector. The uncertainty of this measurement is assumed to be 1.59 mm ( $1/16''$ ). Only a systematic error is considered for this error source. Although random error may exist in this measurement between scans, it is not quantified because this results in a systematic error for each scan. This uncertainty is highest at the vertex and decreases as the laser angle increases.

The laser scanner is leveled before each test with an inclinometer that has an uncertainty of 0.087 mrad. The operator levels the scanner to 0.523 mrad or less before each test. This uncertainty peaks at the vertex and at the outer portions of the aperture and follows the trend in the return-spot location on the target. Figure 8 shows the return-spot location trend on the target. The step change in the laser output angle is constant, but the distance between the return-spot locations is not. The minimum change in distance is where the return spot changes direction (circled in black). The plot on the right is the laser return-spot locations with respect to the output angle. The negative output angles for the laser have positive return-spot locations on the target, and positive laser output angles have negative return-spot locations. The distance from the target to the vertex of the collector is measured with a laser range finder that has an accuracy of  $\pm 1.27$  mm. The slope error uncertainty trend for this is linear and has a positive slope if the distance is below the true value or negative if the distance is above the true value.

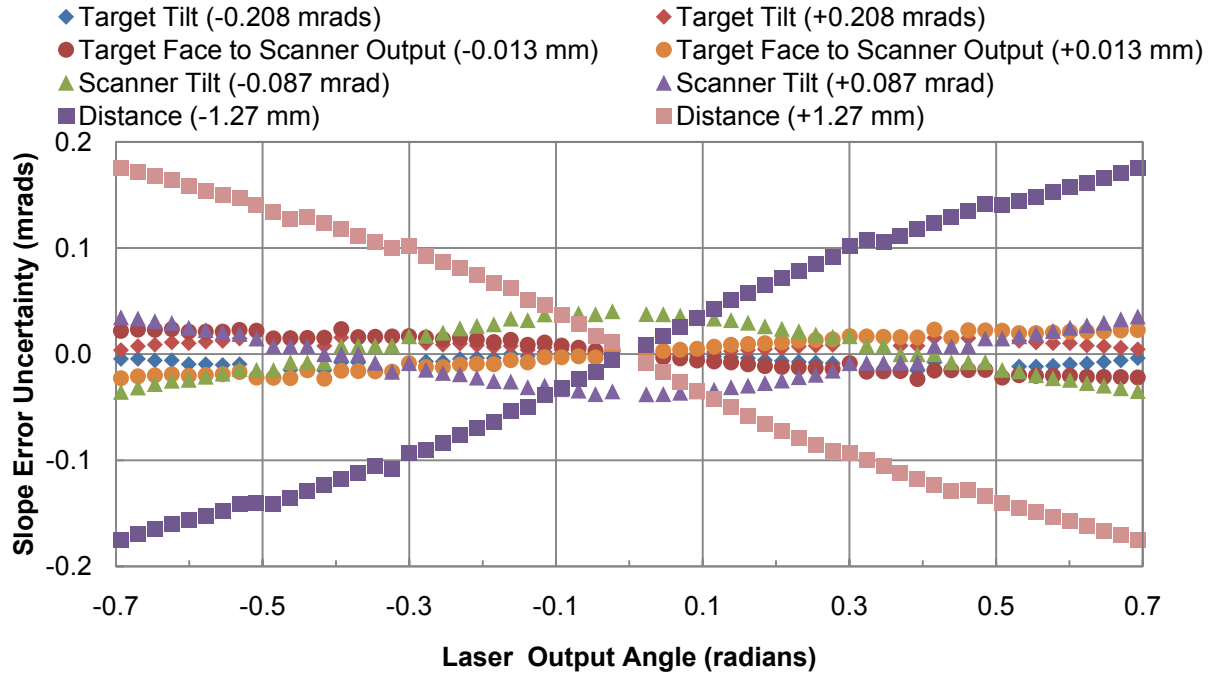


Figure 6. Results from random slope error uncertainties listed in Table. The only uncertainties not shown are the camera and scanner. Resolution errors in the MATLAB program used to generate these results are visible for slope error differences less than 0.01 mrad. The resolution errors cause the slope error trend to appear jagged rather than smooth.

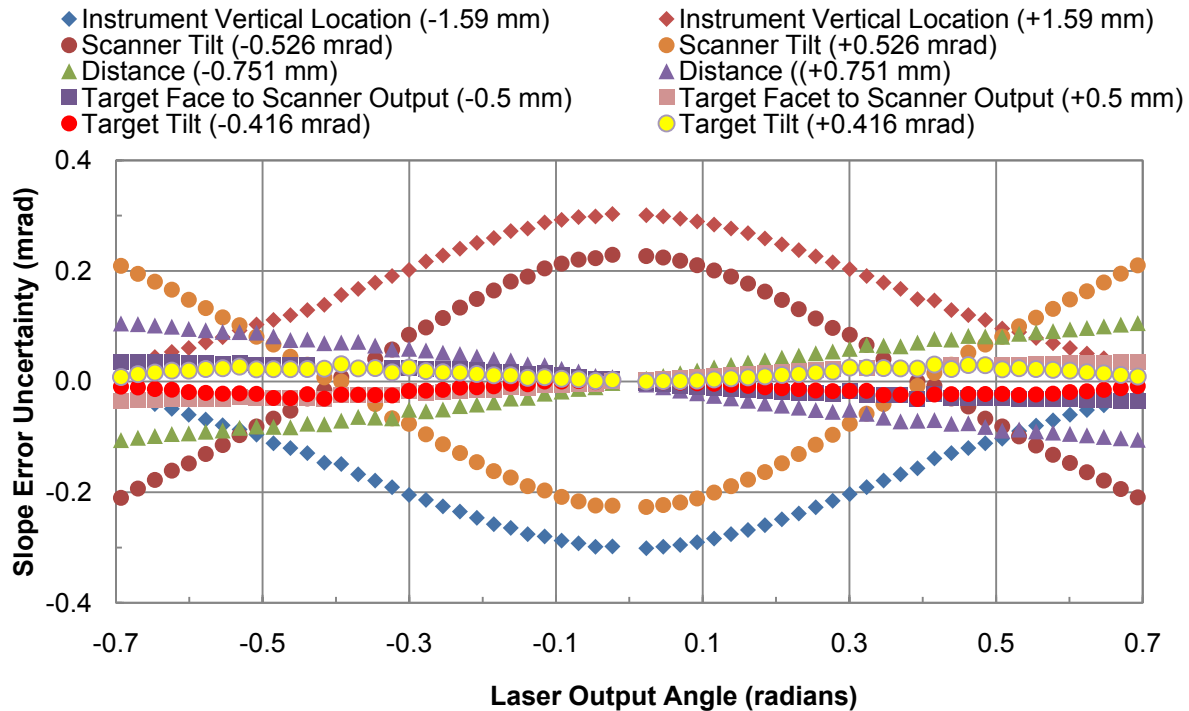
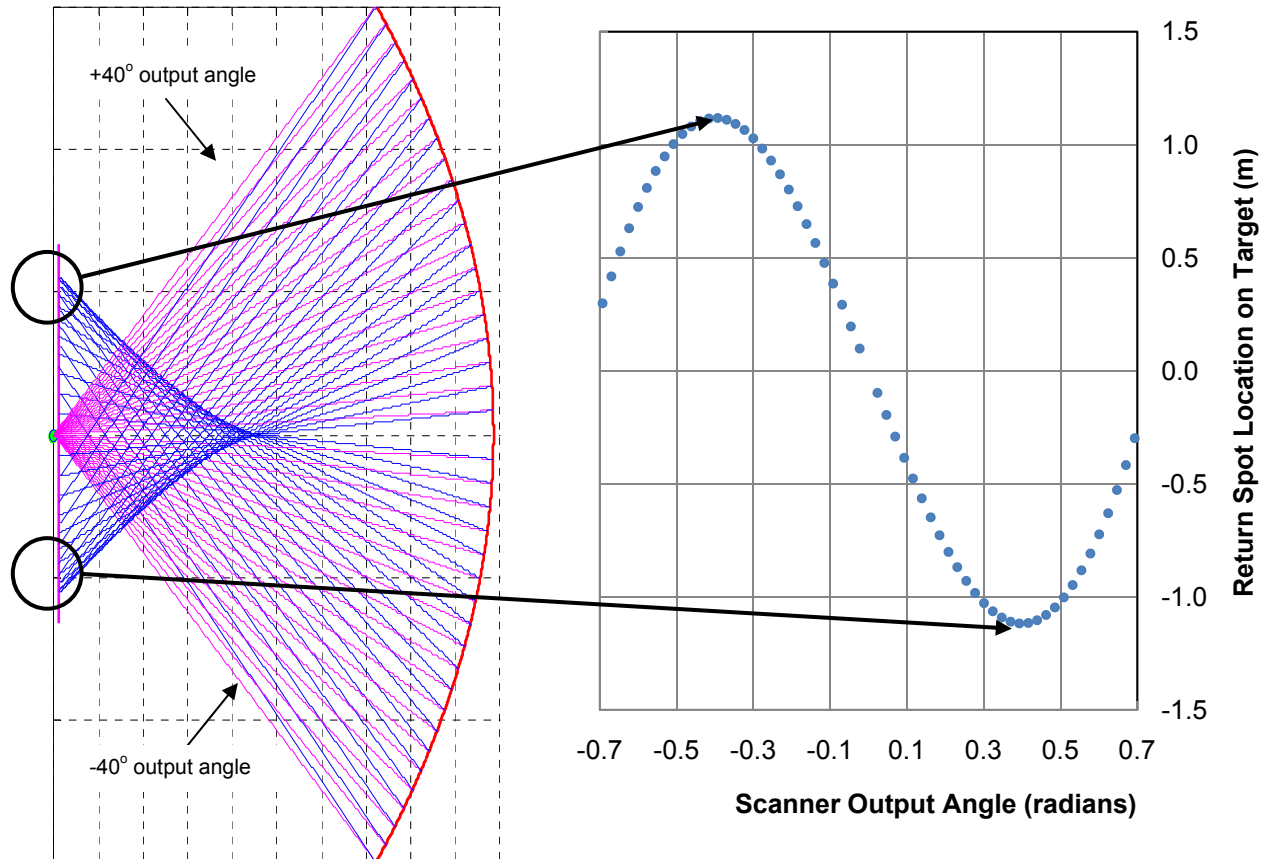


Figure 7. Results from systematic slope error uncertainties listed in Table 2. The only uncertainties not shown in the plot are those of the camera and scanner.



**Figure 8.** The figure on the left shows ray paths while scanning a collector. The laser output rays are shown in magenta and the reflected laser rays in blue. The areas circled in black are for laser output angles of  $\pm 0.36$ – $0.50$  radian and shows where the laser return spot changes directions on the target.

### ***Target Tilt***

During setup and at the beginning of each test, the target is leveled in both the vertical and horizontal directions. This is done by an operator with a bubble level that has a random uncertainty of 0.127 mm (0.005") over a length of 0.61 m (24"), providing a random uncertainty in the level of the target of 0.208 mrad. This random uncertainty causes slope errors ranging from  $\pm 0.000205$  mrad. Figure 9 shows the calculated slope for a perfect parabola as a function of output laser position along the aperture assuming a target tilt angle of  $\pm 0.208$  mrad. The linear regression for this random slope error uncertainty data yields  $dz/dy = 0.2924y \pm 8 \times 10^{-6}$ , with the sum of the squared residuals ( $R^2$ ) equal to 1.00. The slope of the line is 0.2924, resulting in a focal length of 1.71 m. This shows that the random errors in the target tilt have a negligible effect on the calculated focal length. The tilt term is  $8 \times 10^{-6}$  radians, or 8  $\mu$ rad and can be considered a negligible contribution (within the noise of the instrument).

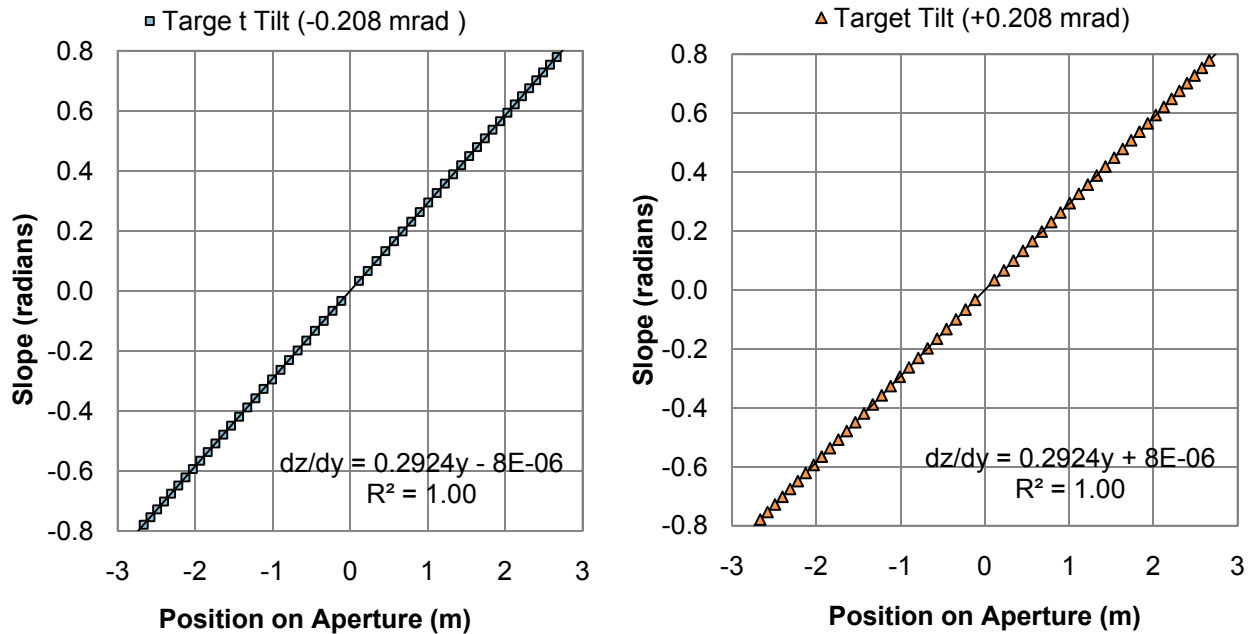


**Figure 9. The calculated slopes along the aperture of a parabola with the target tilted at  $\pm 0.208$  mrad.**

The systematic error for this bubble-level measurement is arbitrarily estimated to be two times the random error or 0.416 mrad. This systematic error is caused by the operator's handling/placement of the instrument, flatness of the target or other sources. The slope errors caused by this systematic uncertainty ranges from 0.0002 to 0.031 mrad. A linear regression of this systematic slope error yields  $dz/dy = 0.2924y \pm 2 \times 10^{-5}$ , with the sum of the squared residuals ( $R^2$ ) equal to 1.00. The slope of the line is 0.2924, resulting in a focal length of 1.71 m. The tilt term is  $2 \times 10^{-5}$  radians, or 0.02 mrad.

### **Target Face to Laser Scanner Output**

The distance between the front of the VSHOT target and the laser scanner output is measured during the setup. This measurement is highlighted in Figure 10 with a thick white line. Calipers are used to measure this distance, and they have a random uncertainty of  $\pm 0.127$  mm. The slope errors caused by this random uncertainty are relatively small, ranging from -0.0235 to +0.0235 mrad across the aperture. A linear regression of the random slope error uncertainty in this measurement yields  $dz/dy = 0.2924y \pm 7 \times 10^{-7}$ , with the sum of the squared residuals ( $R^2$ ) equal to 1.00. The slope of the line is 0.2924, resulting in a focal length of 1.71m. The tilt term is  $7 \times 10^{-7}$  radians, or 0.0007 mrad, and can be considered negligible (within the noise of the instrument).

This measurement has a systematic error of  $\pm 0.5$  mm based on observed consistency among operators making the measurement. The resulting systematic slope error uncertainty is relatively small, ranging between  $\pm 0.0355$  mrad with the absolute minimum at a laser output angle of  $0^\circ$ . Figure 11 shows the calculated slope for a perfect parabola with systematic measurement error of  $\pm 0.508$  mm. A linear regression of these data was completed to determine the effect on the



calculated focal length and tilt. Based on this regression, the focal length matches the design at 1.71 m with a tilt of  $7 \cdot 10^{-7}$  radians, or 0.7  $\mu$ rad, and can be considered negligible.

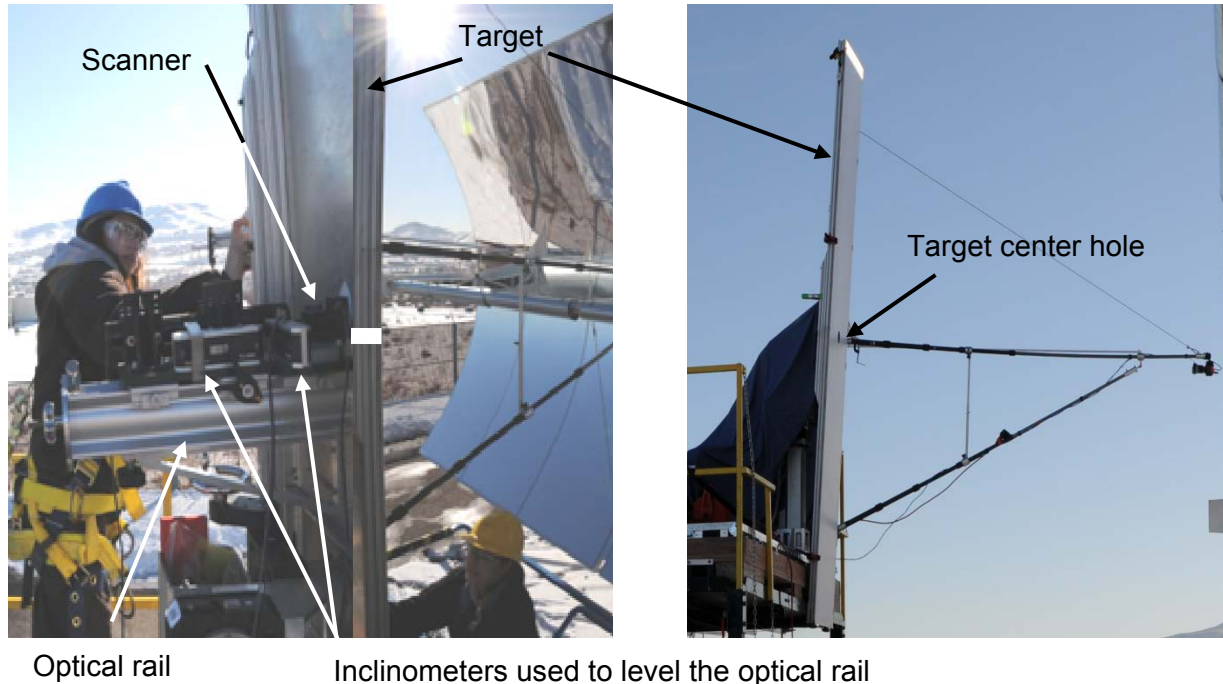


**Figure 10.** The image on the left is the back of the VSHOT TO-GO system. The optical rail is mounted on the back of the target. The image on the right is of the front of the VSHOT TO-GO. The distance between the front of the VSHOT target and the laser scanner output is measured with a caliper and is shown as a thick white line in the center of the left image. This measurement is taken through the center hole in the front of the target to the front of the scanner head behind the target. Design drawings provide the additional distance from the front of the scanner head to the center of the output mirror. (Left credit: PIX 17379) (Right credit: Jen Crawford, NREL)

### ***Instrument Vertical Offset***

Before each test, the VSHOT is aligned to the vertex of the optic being tested. The optical rail and target are leveled using the inclinometers shown in Figure 10. The operator does a visual inspection to make sure the laser (set to zero angle in both x and y) is directed to the vertex of the optic. The vertex point is usually specified by the manufacturer because there is usually no well-defined physical feature at the vertex. Only a systematic error is considered for this measurement. Although a random error may exist between scans, it is not quantified because of the difficulty in the operator's ability to measure the centroid of the laser.

The laser beam is about 6 mm in diameter. We believe that the operator can estimate the center of the laser relative to the vertex of the optic to within 2 mm. This results in a systematic uncertainty in slope error ranging from about 0.02 to 0.30 mrad, with the peak at a laser output angle of zero. The calculated slopes for a perfect parabola with the VSHOT vertical offset at  $\pm 1.59$  mm are plotted in Figure 12. A linear regression calculates the effect of this uncertainty on

the best-fit focal length and tilt term. The best-fit focal length is 1.71 m and the tilt term is  $2 \times 10^{-4}$  radians, or 0.2 mrad.

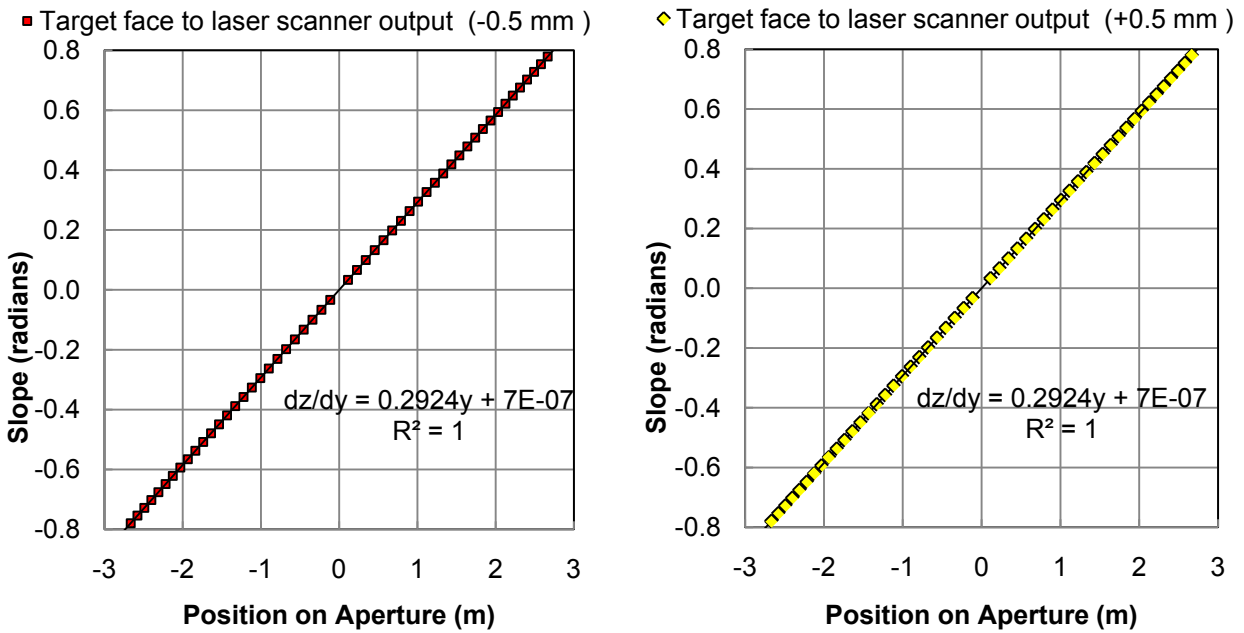


Figure 11. Calculated slope along the aperture of a perfect parabola with target face to laser scanner output mirror distance error of  $\pm 0.508$  mm.

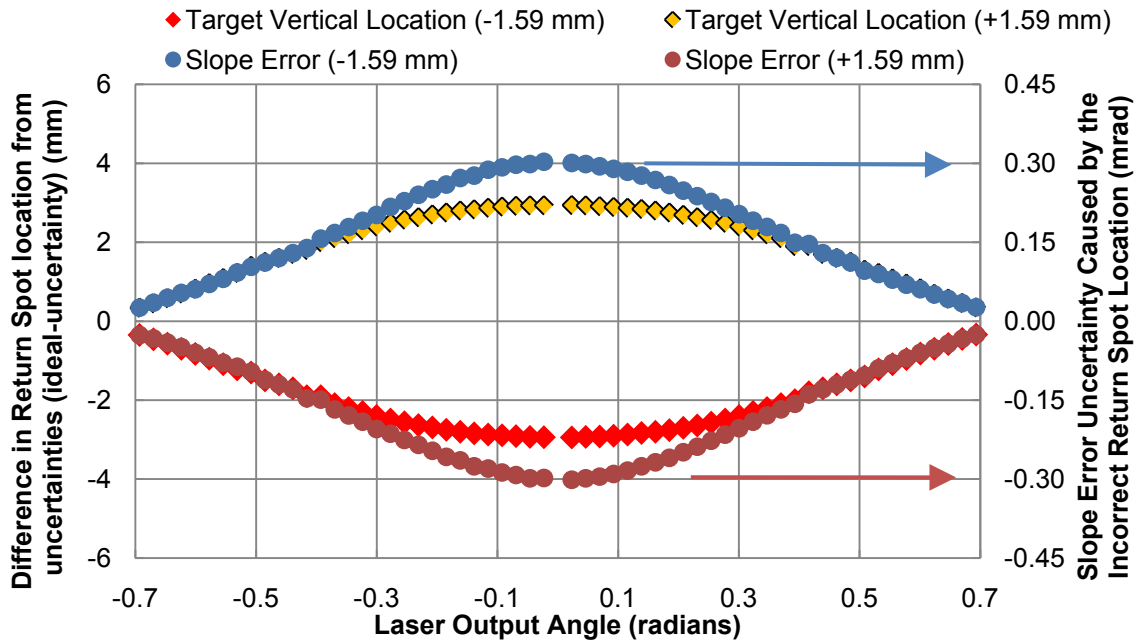
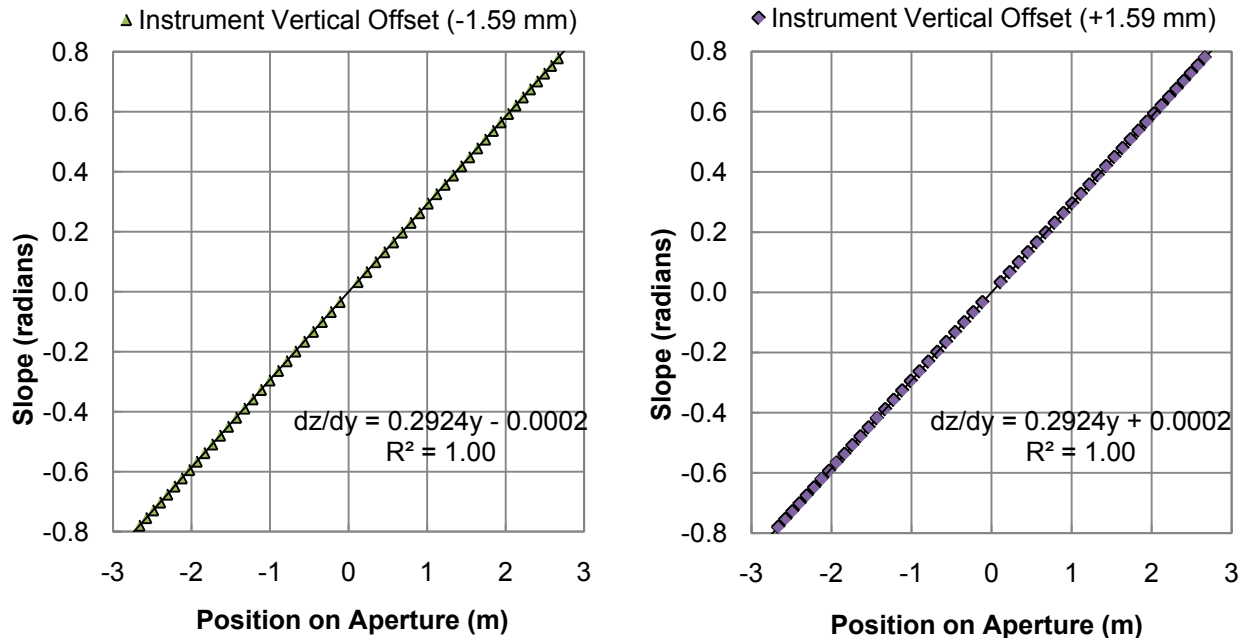


Figure 12. Systematic error caused by the vertical offset of the VSHOT relative to the collector vertex. The vertical axis on the left is the difference in return-spot location on the target caused by the uncertainty at each laser output angle. The vertical axis on the right is the calculated slope error.



**Figure 13. Calculated slopes along the aperture of a perfect parabola with the VSHOT vertical offset of  $\pm 1.59$  mm are plotted in the charts.**

### Scanner Tilt

The scanner is securely fixed to an optical rail which is fixed to the back of the target. The rail also holds the laser in a rigid position and orientation. The inclinometers used to level the scanner and rail assembly have a random uncertainty of 0.009 mrad ( $0.005^\circ$ ). The random uncertainty associated with the scanner tilt peaks at the vertex and at the outer portions of the aperture. This uncertainty follows the trend in the change of return-spot location on the target. The minimum is where the return-spot locations are close together (turn-around points). The maximum and minimum slope errors for this random uncertainty range from  $\pm 0.04$  mrad, depending on the laser output angle. A linear regression was completed on the slope data to estimate the effect of this random uncertainty on the best-fit focal length and tilt term. The linear regression of these data yielded  $dz/dy = 0.2924y \pm 4 \cdot 10^{-6}$ . The best-fit focal length is 1.71 m and the tilt term is  $4 \cdot 10^{-6}$  radians, or 0.004 mrad.

The scanner is leveled to  $\pm 0.523$  mrad ( $0.03^\circ$ ) or less before each test using two inclinometers located on the optical rail (shown in Figure 10). The systematic uncertainty is plotted in Figure 14. The maximum and minimum slope errors for this systematic uncertainty range between  $\pm 0.22$  mrad, depending on the laser output angle. Figure 15 shows two plots of the calculated slopes assuming a laser output angle error of  $\pm 0.524$  mrad. The linear regression performed on these data shows that this uncertainty has a negligible impact on the best-fit focal length and a small impact on the tilt term, 0.03 mrad.

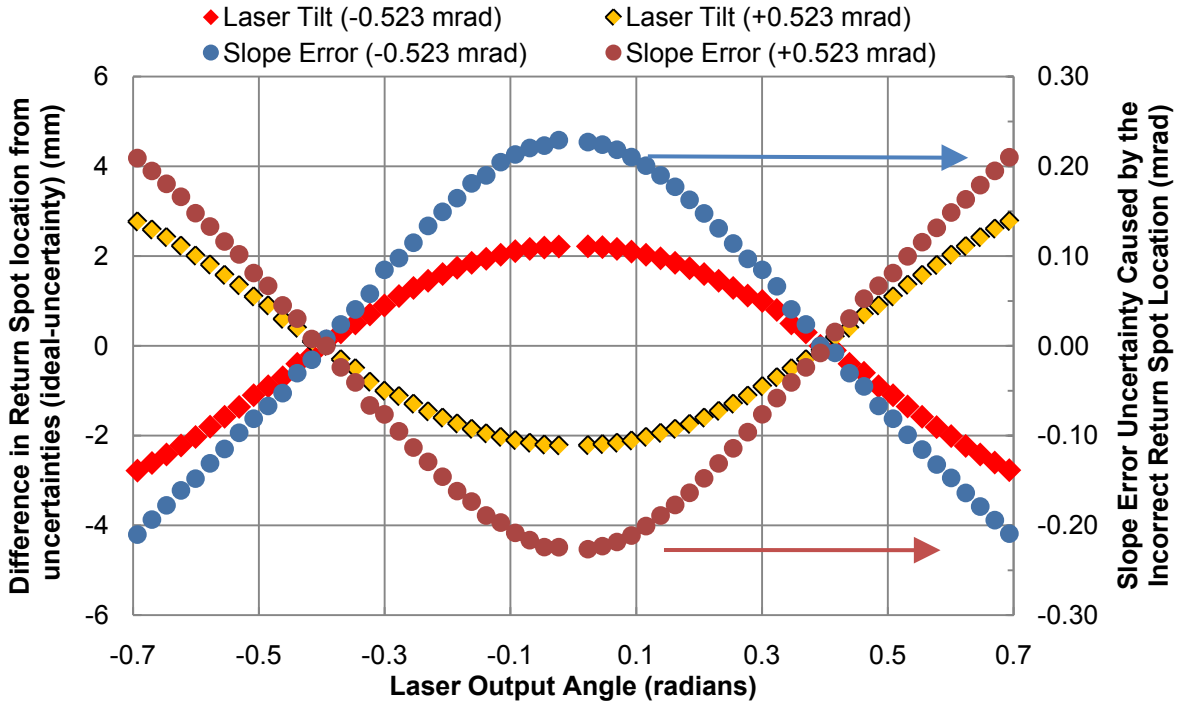


Figure 14. Scanner tilt systematic error for tilt values of  $\pm 0.523$  mrad. The vertical axis on the left is the difference in return-spot location on the target caused by the uncertainty in the laser tilt. The vertical axis on the right is the calculated slope error caused by the error in the return-spot location.

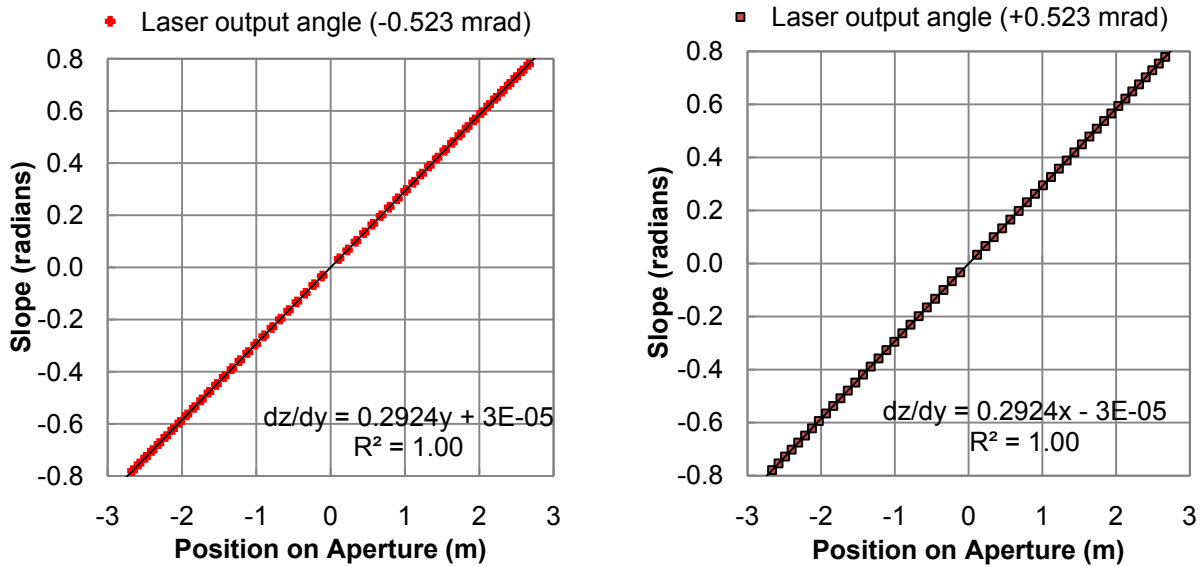


Figure 15. Calculated slopes for a perfect parabola with scanner tilt of  $\pm 0.523$  mrad are plotted.

### Distance from Target to Test Piece

The distance between the VSHOT target and the vertex of the test article is measured before every test. This measurement is taken by an operator with a laser distance range finder that has an accuracy of  $\pm 1.27$  mm (0.05"). This random uncertainty has a linear effect on the return-spot location on the target and leads to a linear effect on the slope errors between  $\pm 0.17$  mrad, as shown in Figure 16. Figure 17 is a plot of the calculated slopes for a perfect parabola with measured distance errors between the target and the test piece of  $\pm 1.27$  mm. A linear regression of this positive and negative random uncertainty slope error data yields  $dz/dy = (0.2924 \pm 0.0001) y \pm 7 * 10^{-7}$ . Using Equation 9 to solve for the focal length results in a 0.6 mm variation in the focal length ( $1.71 \pm 0.0006$  m). This random uncertainty had a negligible impact on the tilt.

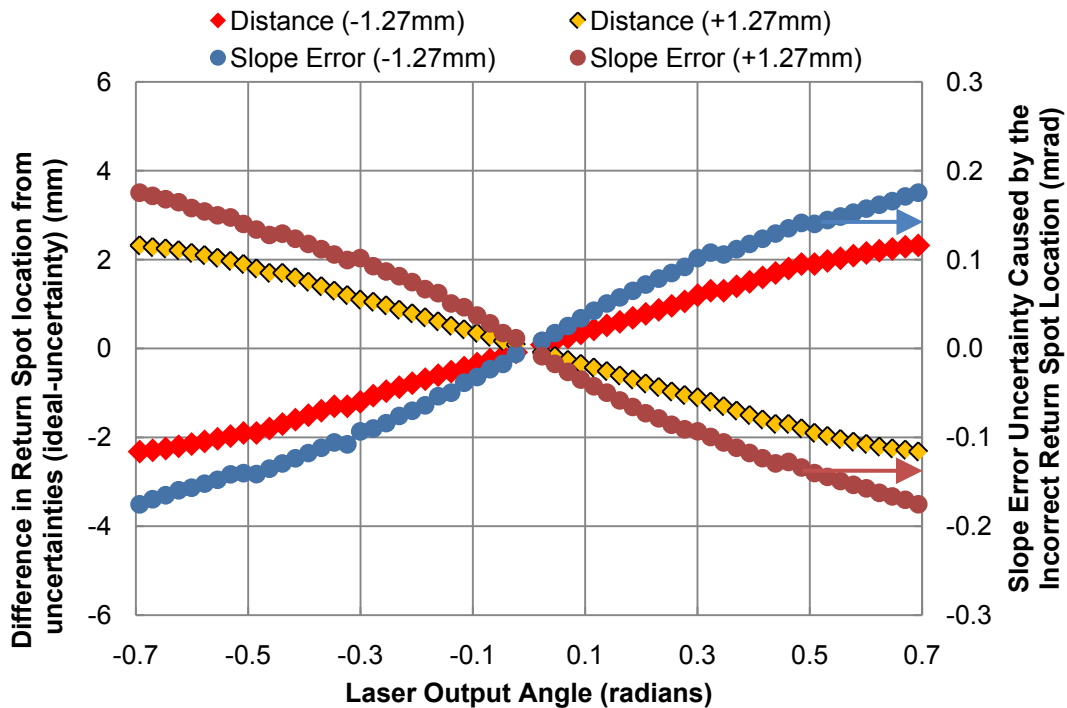
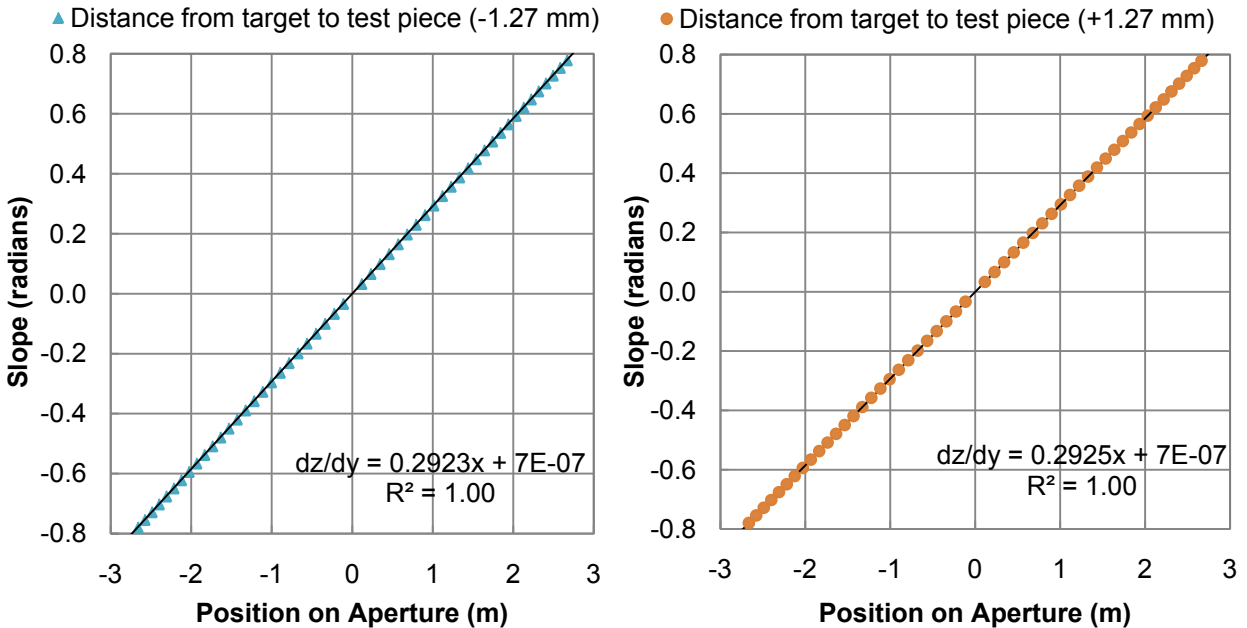
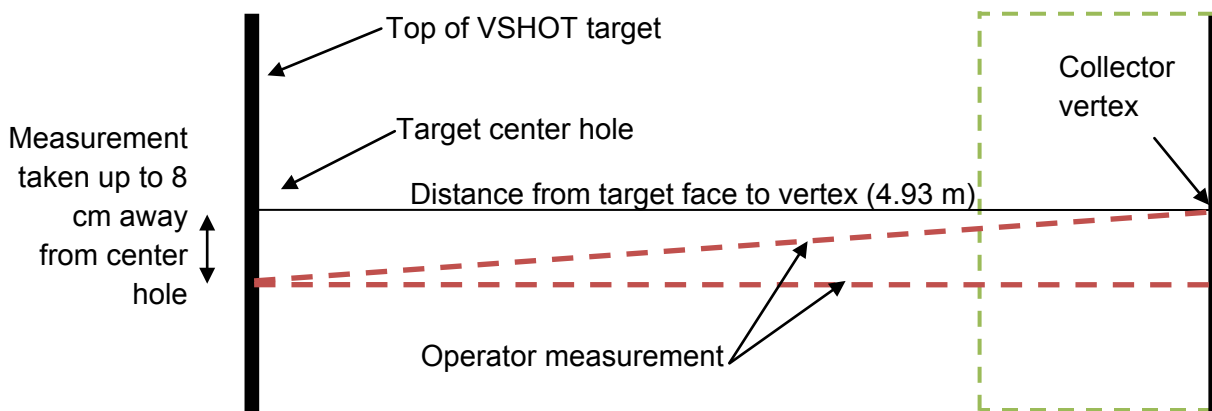


Figure 16. Random errors caused by the laser range finder used to measure the distance between the VSHOT and the vertex. The vertical axis on the left is the difference in return-spot location on the target caused by the uncertainty over the collector. The vertical axis on the right is the calculated slope error associated with the error caused by the error in the return-spot location.



**Figure 17. Calculated slope at multiple points across a collector assuming a  $\pm 1.27$ -mm variation in the distance between the target and test piece.**

This distance measurement is made by an operator before each test. Depending on how the operator makes this measurement, a systematic error can be introduced into the data. The operator takes this measurement by placing the laser range finder in front of the target. It is easy for the operator to slightly angle the laser range finder and measure a distance longer than the actual distance. It is estimated that the operator could angle the laser range finder up to  $0.0175$  radian ( $1^\circ$ ), potentially causing a  $\pm 0.751$ mm ( $0.0300''$ ) systematic error in this measurement. Figure 18 is a top view of the VSHOT relative to a collector. The operator takes the measurement as close to the center of the target as possible.



**Figure 18. Top view of the VSHOT and a collector. The dashed lines between the target and the collector show two ways an operator can measure the distance between the target and the collector vertex.**

The errors caused by the systematic uncertainty follow the same trend as the random uncertainties except the errors are smaller. The slope error trend is linear, with a maximum at +0.11 mrad and a minimum of -0.11 mrad. A linear regression was performed on the systematic slope error data to determine its effect on the focal length and tilt. A linear regression of these data yielded  $dz/dy = 0.2924y \pm 7 \cdot 10^{-7}$ , with the sum of the squared residuals ( $R^2$ ) equal to 1.00. Equation 9 was used to calculate a focal length of 1.71 m. The error in focal length at this level of systematic error is negligible.

### **Camera Calibration**

The camera must be calibrated so that pixel space can be related to actual xy space on the target. This is done during setup once the camera location, orientation, lens focal length and focus are fixed. The camera is calibrated using the calibration grid shown in Figure 2. The calibration grid has 46 dots in the vertical direction and 7 dots in the horizontal. The diameter of the dots is 63.5 mm (2.50") and they are spaced 76.2 mm (3.00") apart. Twelve camera-calibration files taken over recent VSHOT testing history were used to estimate the uncertainty in the typical camera calibrations.

To estimate the random errors in the camera, we evaluated the number of pixels between the center of each circle. The number of pixels between circle centers was divided by the known distance, 76.2 mm (3.00"). This provided an estimate for the variation in pixel response over 76.2 mm. The area of the target used for testing can vary slightly depending on the aperture and focal length of the collector being tested, lens focal length and camera position. For the twelve camera calibrations used in this study, the calibration region ranged from 35 to 43 spots in the vertical direction and 5 spots in the horizontal. The regions of the target that are typically used are shown in Figure 19. As the calibration region increases, the pixels per area decrease. This is expected because the number of pixels in the camera is fixed. The number of pixels/mm ranged from 0.54 to 0.68. The data sets from each calibration file were normalized by scaling the dataset with respect to their mean values. The normalized number of pixels/mm was  $0.673 \pm 0.038$  ( $2\sigma$ ). One pixel thus corresponds to 1.49 to 1.57 mm on the target. Figure 20 is a plot of this uncertainty. Errors in return-spot location range from  $\pm 0.7$  mm. Slope errors range from  $\pm 0.07$  mrad.

The positive random uncertainty for the camera uses less pixels per area than the negative. This reduces the camera's ability to image the calibration spots (and the laser during testing), increasing the uncertainty. This appears to have a random effect on the slope error trend over the aperture. This is expected because determining the laser location on the target is limited to 1.41 and 1.57 mm/pixel. An example of this effect is shown in Figure 21.

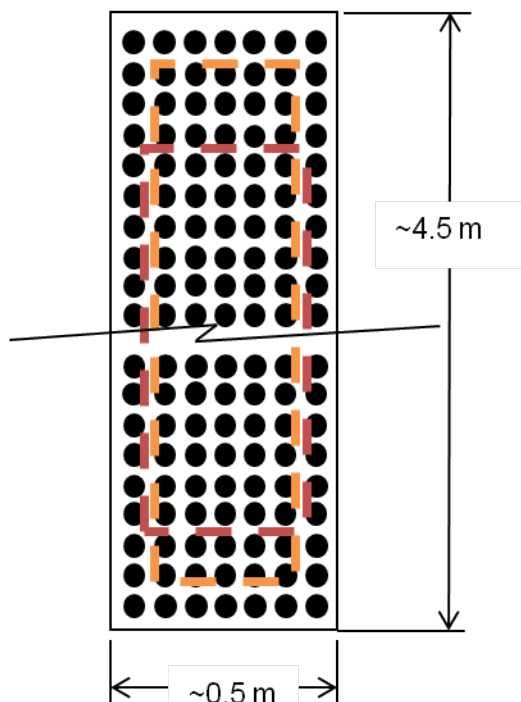


Figure 19. Drawing of the camera calibration target. The dashed lines represent two common camera calibration regions that are used for trough testing.

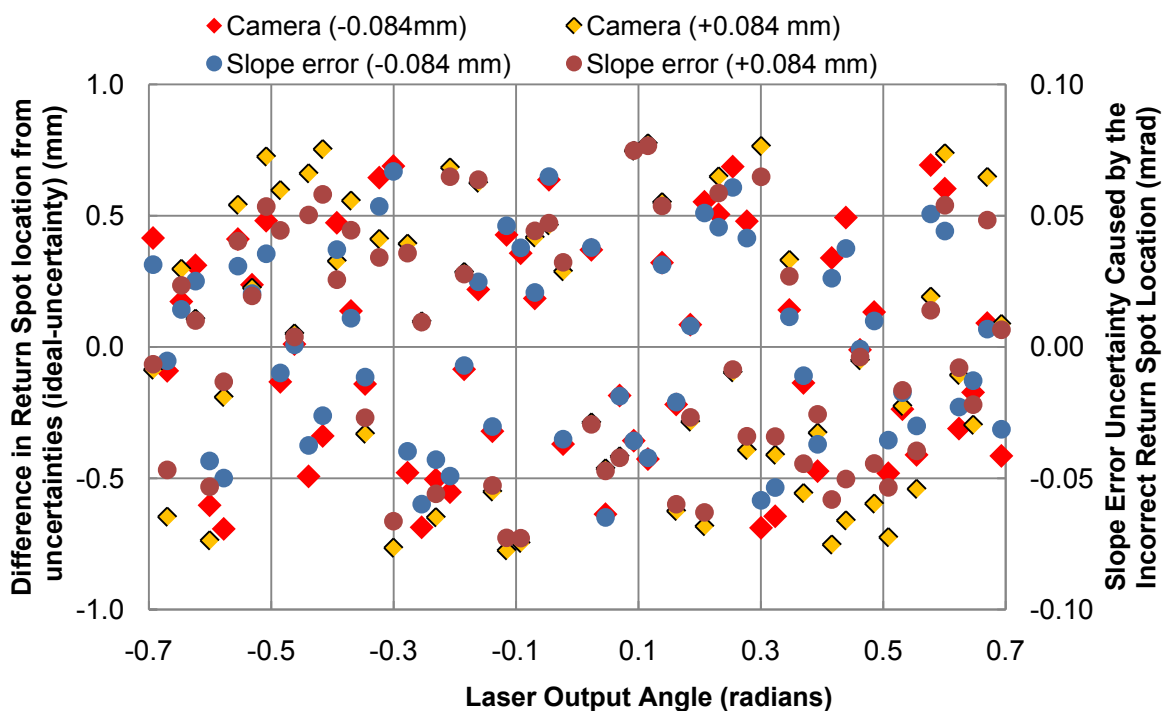
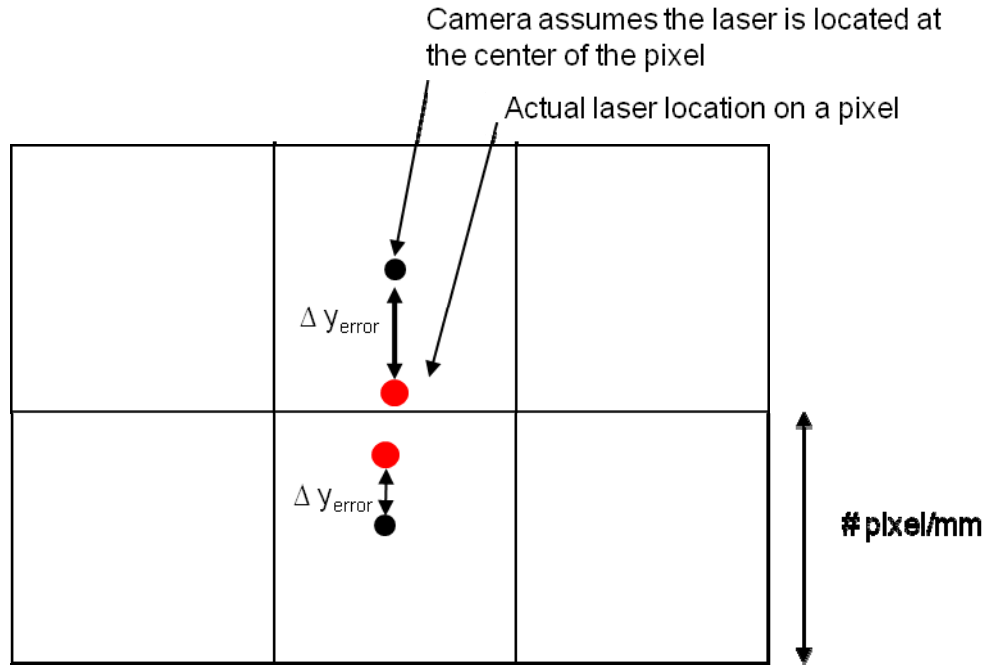


Figure 20. Plot of the random error in the camera's ability to centroid. The vertical axis on the left is the difference in return-spot location on the target caused by the uncertainty over the collector. The vertical axis on the right is the calculated slope error associated with the error caused by the error in the return-spot location.



A linear regression was performed on the calculated slopes across a perfect collector assuming a camera random uncertainty of 1.41 and 1.57 mm. This data set (not shown in a figure) yields  $dz/dy = 0.2924 y + 5 \cdot 10^{-7}$  and  $dz/dy = 0.2924 y + 7 \cdot 10^{-7}$ , with the sum of the squared residuals ( $R^2$ ) equal to 1.00. The slope of the line is 0.2924 and using Equation 9 to calculate the focal length results in a 1.71-m focal length. The tilt term is  $5 \cdot 10^{-7}$  radian, or 0.5  $\mu$ rad, and  $7 \cdot 10^{-7}$  radian, or 0.7  $\mu$ rad, and both can be considered negligible.



**Figure 21. Drawing of camera to target response in pixel/mm (boxes correspond to a camera pixel). Errors in the camera’s ability to locate the laser increase as the number of mm increase per pixel.  $\Delta y_{error}$  is the error in locating the laser on the target. The larger (red) dot is where the laser is striking the target. When the camera images this, it assumes the laser is in the center, not the lower edge, causing an error in the measured return-spot location. This effect causes the random error effects shown in Figure 20 and 22.**

The same twelve camera-calibration files were used to estimate the systematic uncertainty. Based on previous VSHOT experience the standard deviation in the camera calibration errors for x and y directions should be less than 0.381 mm (0.015”). The standard deviation of each file is listed in Table 3. Each file has a standard deviation for each direction. To get an estimate for standard deviation over all the data sets, the individual standard deviations were pooled. Using Equation 10, with  $\nu_i$  equal to the degrees of freedom in the calibration.  $S_{x,i}$  and  $S_{y,i}$  are the standard deviation in the x and y direction associated with the data set. Systematic errors in this study have a 95% confidence, or  $2\sigma$ . The camera calibration systematic error is 0.374 mm ( $2\sigma$ ) from Table 3.

**Table 3. Camera calibration files used to estimate the systematic uncertainty. The degrees of freedom,  $v_i$ , and standard deviation in the x and y direction are listed.**

| File Number                                                                                                         | $v_i$ | $S_{X,i}$ (x-direction) |       | $S_{Y,i}$ (y-direction) |              |
|---------------------------------------------------------------------------------------------------------------------|-------|-------------------------|-------|-------------------------|--------------|
|                                                                                                                     |       | mm                      | in    | mm                      | in           |
| 1                                                                                                                   | 204   | 0.076                   | 0.003 | 0.102                   | 0.004        |
| 2                                                                                                                   | 184   | 0.051                   | 0.002 | 0.076                   | 0.003        |
| 3                                                                                                                   | 174   | 0.076                   | 0.003 | 0.076                   | 0.003        |
| 4                                                                                                                   | 174   | 0.025                   | 0.001 | 0.076                   | 0.003        |
| 5                                                                                                                   | 184   | 0.152                   | 0.006 | 0.127                   | 0.005        |
| 6                                                                                                                   | 184   | 0.076                   | 0.003 | 0.127                   | 0.005        |
| 7                                                                                                                   | 184   | 0.051                   | 0.002 | 0.152                   | 0.006        |
| 8                                                                                                                   | 185   | 0.330                   | 0.013 | 0.305                   | 0.012        |
| 9                                                                                                                   | 174   | 0.076                   | 0.003 | 0.152                   | 0.006        |
| 10                                                                                                                  | 184   | 0.076                   | 0.003 | 0.127                   | 0.005        |
| 11                                                                                                                  | 194   | 0.051                   | 0.002 | 0.102                   | 0.004        |
| 12                                                                                                                  | 300   | 0.102                   | 0.004 | 0.127                   | 0.005        |
| <b>Pooled Standard Deviation (<math>\sigma</math>), includes both <math>S_{X,i}</math> and <math>S_{Y,i}</math></b> |       |                         |       | <b>0.187</b>            | <b>0.007</b> |

$$S_{pooled} = \left[ \frac{\sum_{i=1}^N v_i \left[ (S_{X,i})^2 + (S_{Y,i})^2 \right]}{\sum_{i=1}^N v_i} \right]^{1/2} \quad \text{Equation 10}$$

The slope error trend over the aperture resembles a scatter plot. This is expected because determining the laser location on the target is limited to 0.374 mm ( $2\sigma$ ) and this effect is illustrated in Figure 21. Figure 22 is a plot of this uncertainty. Errors in return-spot location range from  $\pm 0.2$  mm. Slope errors range from  $\pm 0.02$  mrad. Linear regression of this slope data is plotted in Figure 23 and yields  $dz/dy = 0.2924y \pm 7 \cdot 10^{-7}$  with the sum of the squared residuals ( $R^2$ ) equal to 1.00. Equation 9 was used to calculate a focal length of 1.71 m. The tilt term is 0.0007 radians, or 0.7  $\mu$ rad.

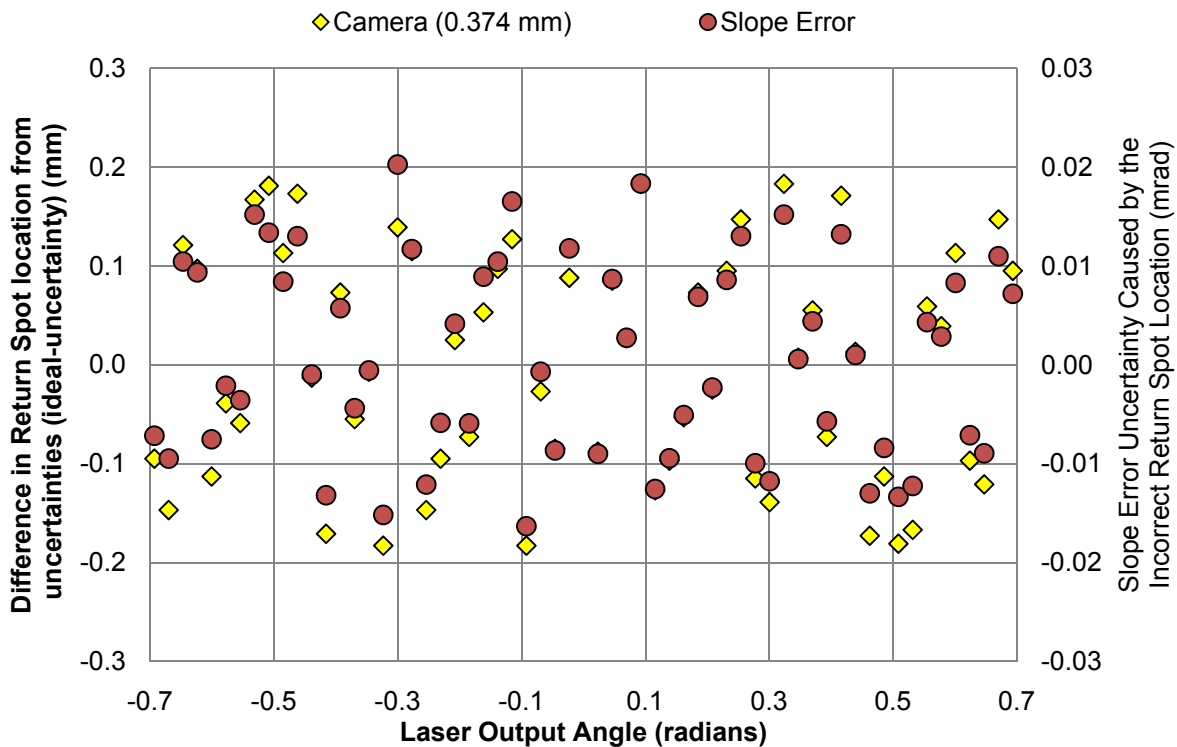


Figure 22. Systematic uncertainty in the camera calibration. The vertical axis on the left is the difference in return-spot location on the target caused by the uncertainty in the laser tilt. The vertical axis on the right is the calculated slope error caused by the error in the return-spot location.

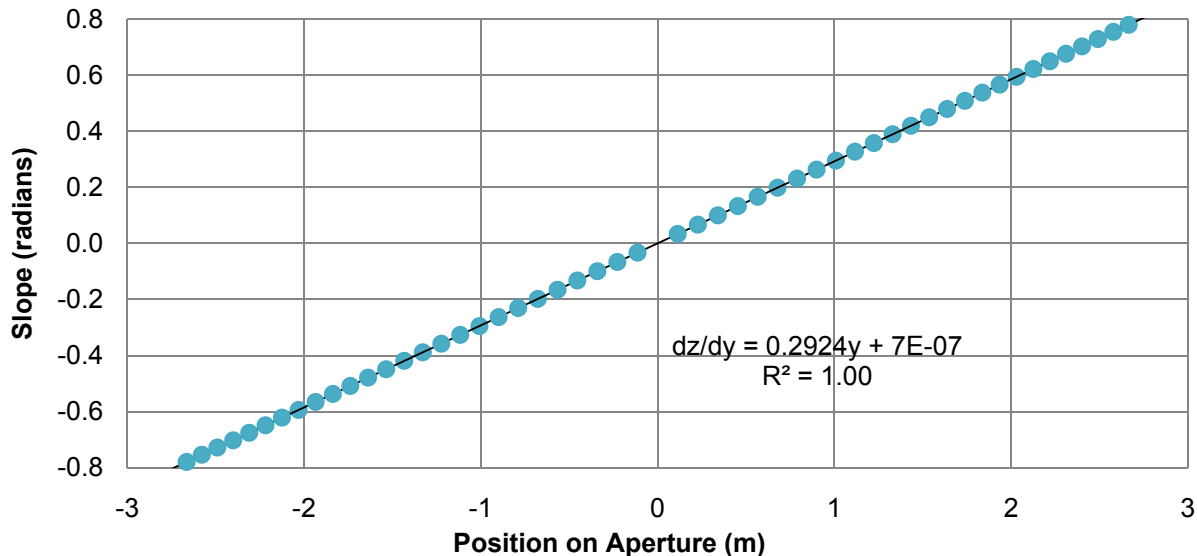


Figure 23. Calculated slope at multiple points across an ideal parabola with a 6-m aperture and 1.71-m focal length accounting for a systematic uncertainty of 0.374 mm is plotted.

When using VSHOT to test outdoors, the system setup is completed during the day and testing is done at night. The target is made of aluminum honeycomb. The calibration spots are printed on a plastic foam core that has been bonded to the front side of the target. The target could potentially expand or contract from the time of setup to testing. This expansion is expected to be less than our ability to measure it; therefore, it is not expected to contribute to the uncertainty. However, before the camera is calibrated, the distance between calibration spots on the target is measured with calipers in a few selected areas. This is a precautionary measure to make sure nothing has happened to the target since the last time it was used. After this measurement is completed, the camera is calibrated.

A white target is then placed over the calibration grid to make the contrast between the target and laser easily distinguishable for both the camera and operator. The aperture on the camera is reduced so that it no longer images any stray light on the target and can only image the laser. If the dimensions of the target change during testing at night because of thermal expansion or contraction, it will not have any effect on the camera's ability to locate the return-spot location. This is because during testing the camera does not use the target as a reference for relating pixel space to xy space. The location of the return spot in xy space is based on the camera calibration that was performed immediately after the calibration grid was inspected. There could be other temperature related impacts on the VSHOT assembly (e.g. thermal expansion on the camera support arms) that are not accounted for in this analysis.

### Scanner/Calibration

The scanner is used to direct the laser beam to the different angles across a test piece. The laser is mounted to a fixed location and orientation on the optical rail (Figure 24). The laser beam is directed to the x mirror that reflects the laser to the y mirror. At the y mirror, the laser is reflected in the direction of the test piece. The maximum output range of the scanner is 1.38 radian ( $80^\circ$ ).

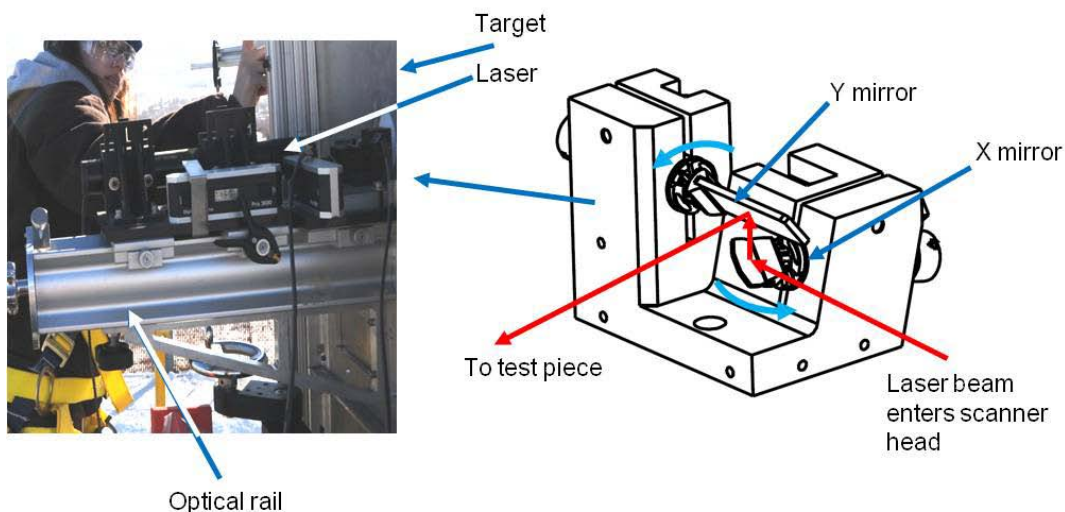


**Figure 24.** The image on the left is the optical rail mounted on the target. The laser is mounted to the top of the rail in a fixed location perpendicular to the target. The scanner is on the top right side of the rail. The drawing on the right shows the basic geometry and hardware for the laser scanner [4]. (PIX 17379)

The laser scanner has two 16-bit closed-loop galvanometers. One rotates to change the laser output angle in the x direction and the other is for the y. According to the manufacturer, the random error in the scanner is  $8 \mu\text{rad}$  [4]. This random error has an extremely small effect on the slope errors across the aperture ranging from  $\pm 4 \mu\text{rad}$ . This has a negligible effect on the calculated focal length and tilt term.

The scanner must be calibrated so that the galvanometer encoder counts can be correlated to angular space when it is mounted on the optical rail. Multiple components are attached to the optical rail and each one may be mounted in a slightly different position than ideal, causing systematic errors in the setup. To minimize this systematic error, the scanner is calibrated using a calibration grid (Figure 25). The scanner calibration grid has a checkerboard pattern on it to assist the operator to determine the laser calibration points. Each square is  $0.241 \text{ m}$  ( $9.50''$ ) long on each side, and each corner represents a laser calibration point. A 12-by-12 grid of points is used to calibrate the scanner. The calibration is performed periodically in the laboratory with the assumption that there are no changes to the calibration with setup and operation in the field.

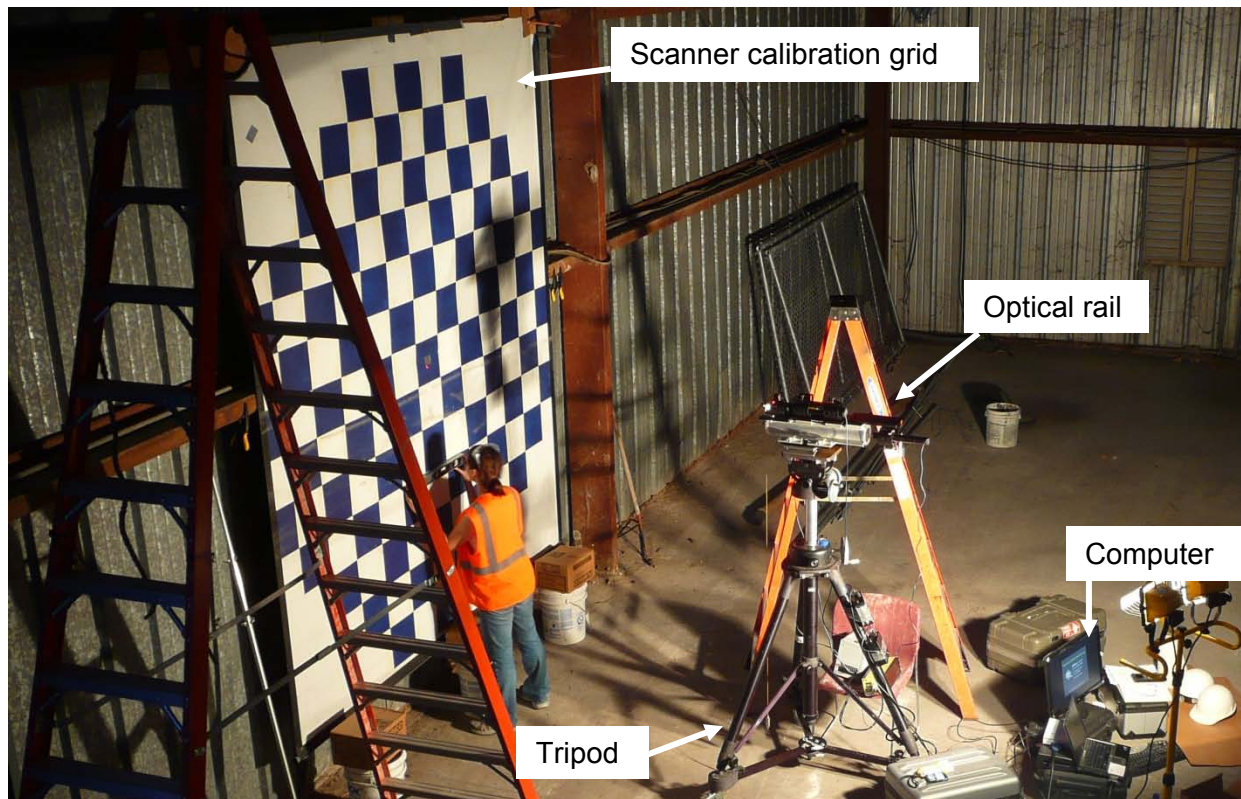


**Figure 25. Image of the scanner being calibrated. The scanner calibration target is mounted on a wall and leveled. The optical rail is mounted on a tripod and centered in front of the target. (credit: Mark Bernardi, NREL)**

Five calibration files were used to estimate the systematic errors in the scanner calibration. Table 4 lists the standard deviation errors for the scanner calibration in the x and y directions. Testing should not be done with errors higher than  $1 \text{ mrad}$  in either direction because this can cause slope error uncertainties larger than  $0.35 \text{ mrad}$ . The error in the x direction of file 4 is

significantly higher than any of the other files, with standard deviation of 5.41 mrad. The error in the x direction for file 3 is also too high, with a standard deviation of 1.30 mrad. If errors this high occur in the scanner calibration, the setup should be checked and the calibration redone.

To estimate the standard deviation over all the data sets, the individual standard deviations were pooled. Equation 10 was used to pool the standard deviations, with  $\nu_i = 144$ , as degrees of freedom in the calibration, and  $S_{X,i}$  and  $S_{Y,i}$  as the standard deviation in the x and y direction. Systematic error associated with the scanner calibration does not include files 3 and 4. The standard deviation,  $\sigma$ , in the scanner calibration is 0.31 mrad. The systematic error in the scanner calibration with 95% confidence ( $2\sigma$ ) is 0.62 mrad.

**Table 4. Standard deviation errors in the scanner calibration. The degrees of freedom,  $\nu_i$ , for each scanner calibration is 144 (12 x 12 grid).**

| File Number                                                                          | $S_{X,i}$ ( x-direction) | $S_{Y,i}$ (y-direction) |
|--------------------------------------------------------------------------------------|--------------------------|-------------------------|
|                                                                                      | X (mrad)                 | Y (mrad)                |
| 1                                                                                    | 0.442                    | 0.509                   |
| 2                                                                                    | 0.141                    | 0.183                   |
| 3                                                                                    | 1.30                     | 0.413                   |
| 4                                                                                    | 5.41                     | 0.561                   |
| 5                                                                                    | 0.191                    | 0.194                   |
| <b>Pooled Standard Deviation (all files)</b>                                         |                          | <b>1.79</b>             |
| <b>Pooled Standard Deviation (<math>\sigma</math>)<br/>(excluding files 3 and 4)</b> |                          | <b>0.31</b>             |

Figure 26 is a plot of the systematic errors in the scanner calibration. Errors in return spot location range from  $\pm 3.3$  mm. Slope errors range from  $\pm 0.25$  mrad. A linear regression was done on the calculated slopes across the aperture to determine its effect on the focal length and tilt. These data yielded  $dz/dy = 0.2924y \pm 3 \cdot 10^{-5}$ , with the sum of the squared residuals ( $R^2$ ) equal to 1.00. The tilt term is of  $3 \cdot 10^{-5}$  radians, or 0.03 mrad.

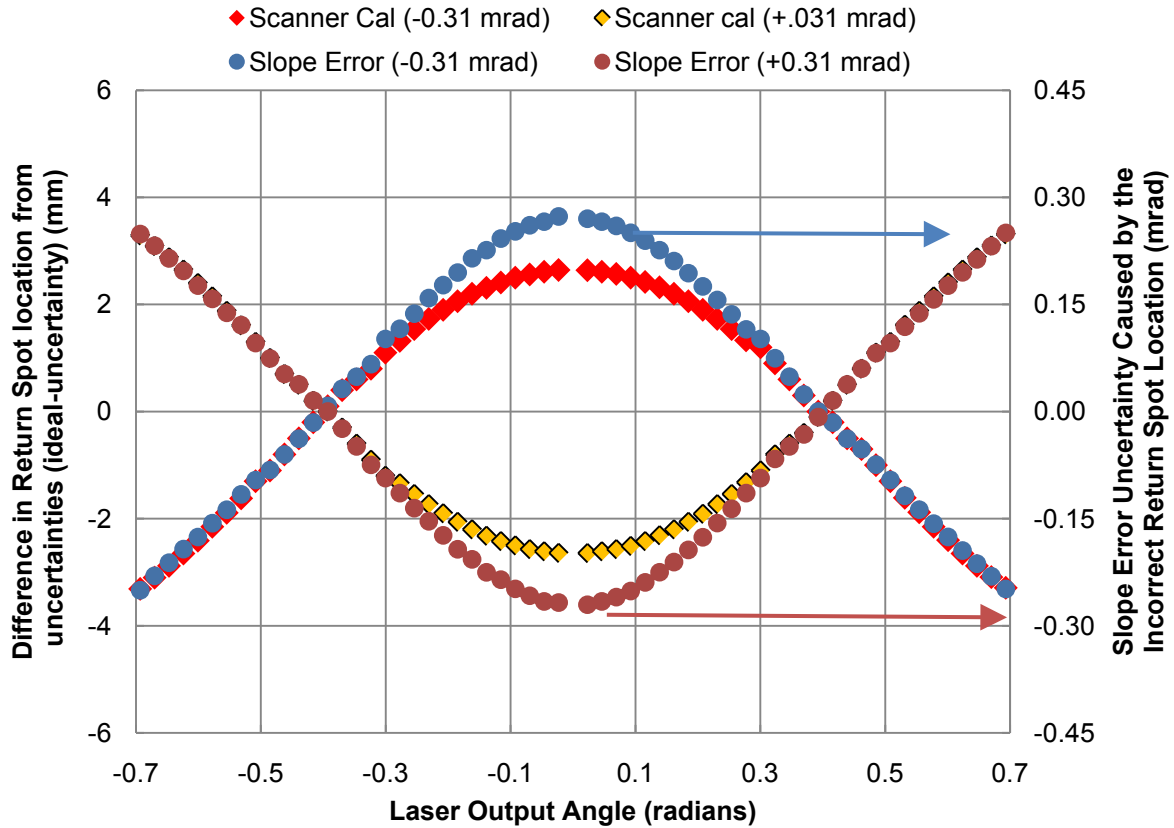


Figure 26. Scanner calibration systematic errors. The vertical axis on the left is the difference in return-spot location on the target caused by the uncertainty in the laser tilt. The vertical axis on the right is the calculated slope error caused by the error in the return-spot location.

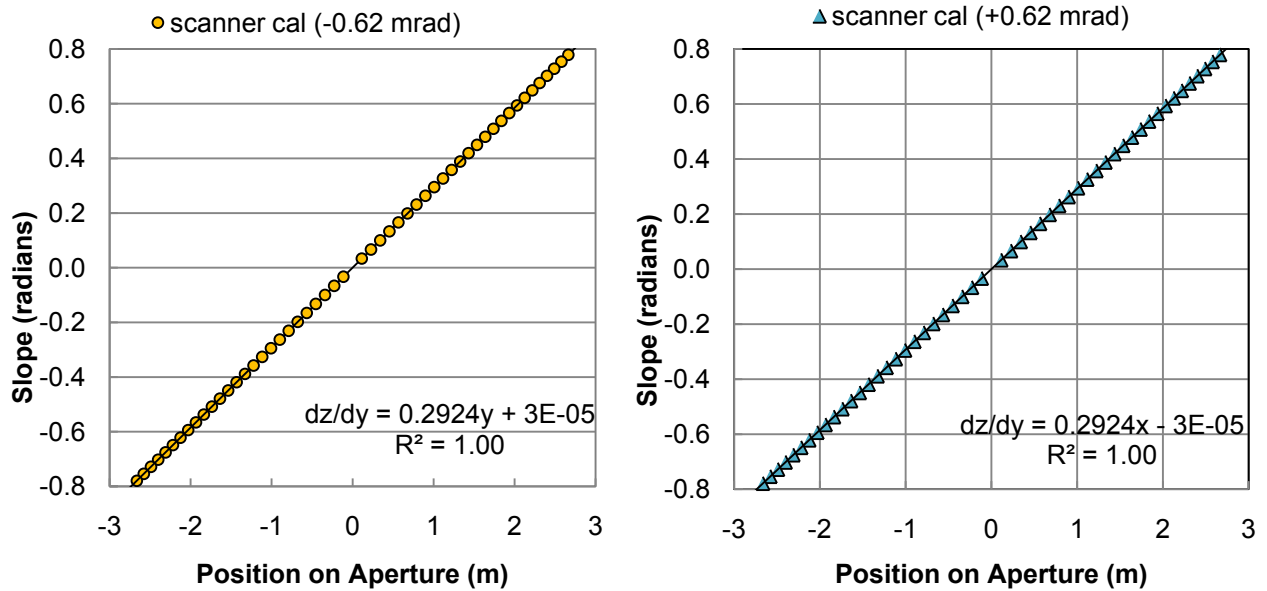


Figure 27. Calculated slopes for a perfect parabola with scanner calibration error of  $\pm 0.62$  mrad are plotted in the charts.

The performance of the scanner as a function of temperature is unknown to the manufacturer and is not considered in this study. The manufacturer guarantees the repeatability to be 8  $\mu$ rad from 0°–50°C and does not recommend operation outside of this range. For this study, we assumed that the scanner is only being operated within this temperature range because no testing has ever been done outside this range. No information is known regarding the effect of relative humidity on the scanner performance. However, the manufacturer does not expect the performance to change and thus it is not considered in this study.

### Uncertainty Estimate – Slope Error

All of the uncertainties considered in this study are for  $2\sigma$  or 95% confidence around the true measurement. Each of the slope error uncertainties and their relative percentage contribution are listed in Table 5 and 6. The slope uncertainty over the laser cone angle varies depending on the output angle of the laser, intersection location on the collector, and return-spot location on the target.

The uncertainties are assumed to be independent of each other and have Gaussian distributions. All of the uncertainties, except for the camera calibration, are assumed to be symmetric about the true value. The systematic standard uncertainty,  $U_S$ , is used to estimate the combined effect of systematic errors ( $U_{S,i}$ ) on slope error test results (Equation 11). The random standard uncertainty,  $U_R$ , is used to estimate the combined effect of random errors ( $U_{R,i}$ ) on slope error test results (Equation 12). The effects on the slope error from these random and systematic uncertainties are shown in Figures 28, 29, and 30.

$$U_S = \left( \sum_{j=1}^M U_{S,i}^2 \right)^{\frac{1}{2}} \quad \text{Equation 11}$$

$$U_R = \left( \sum_{i=1}^N U_{R,i}^2 \right)^{\frac{1}{2}} \quad \text{Equation 12}$$

Six random uncertainties were considered in this study ( $N=6$ ): the measurement of the tilt in the target, distance between the target face and scanner, scanner tilt, distance between the target face and collector vertex, camera calibration, and scanner/calibration. The measured distance between the target face to the test piece had the largest effect on the positive and negative random error,  $\sim 70\%$  for both the positive and negative (Table 5), contributing up to 0.17 mrad of slope uncertainty. The camera calibration was the second largest contributor on the positive and negative random uncertainty, causing up to 0.05 mrad of slope error uncertainty at some angles (Figure 28 and Figure 29). On average, the random camera calibration errors contribute 14%–20% of the total error, with the magnitude depending on whether the uncertainty is positive or negative. Note in Figure 28 and Figure 29 that there are some deterministic effects that depend



on specific output angles where the return position falls within either the upper or lower portion of a camera pixel (see the earlier section on Camera Calibration and Figure 21 for more detail).

**Table 5. Random error contributions to the random slope error uncertainty. The random error in the camera calibration is not symmetrical, so negative and positive random errors for both were calculated.**

| Description                         | Average Contribution to the Uncertainty (%) |             | Maximum Contribution to the Uncertainty (%) |             | Minimum Contribution to the Uncertainty (%) |             |
|-------------------------------------|---------------------------------------------|-------------|---------------------------------------------|-------------|---------------------------------------------|-------------|
|                                     | $U_{R,i}^-$                                 | $U_{R,i}^+$ | $U_{R,i}^-$                                 | $U_{R,i}^+$ | $U_{R,i}^-$                                 | $U_{R,i}^+$ |
| Target tilt                         | 0.5                                         | 0.6         | 1.9                                         | 2.4         | 0                                           | 0           |
| Target face to laser scanner output | 1.7                                         | 1.4         | 3.7                                         | 3.0         | 0.1                                         | 0.1         |
| Scanner tilt                        | 9.8                                         | 7.6         | 58.8                                        | 59.9        | 0                                           | 0           |
| Distance from target to test piece  | 73.1                                        | 70          | 97.9                                        | 95.3        | 1.2                                         | 3.2         |
| Camera calibration                  | 14.7                                        | 20.2        | 70.8                                        | 69.1        | 0                                           | 0.1         |
| Scanner/calibration                 | 0.2                                         | 0           | 1.3                                         | 0.5         | 0                                           | 0           |

To decrease the impact of random errors, the measured distance between the target face and collector vertex and the camera resolution must be improved. The distance between the target face and collector vertex is measured with a laser range finder that has an accuracy of 1.27 mm. A laser range finder with an accuracy of less than 1 mm would be needed to reduce the errors caused by this measurement. A camera with greater resolution would be needed to reduce the camera random errors. This would increase the number of pixels per area and improve the software’s ability to accurately calculate the centroid of the return laser on the target.

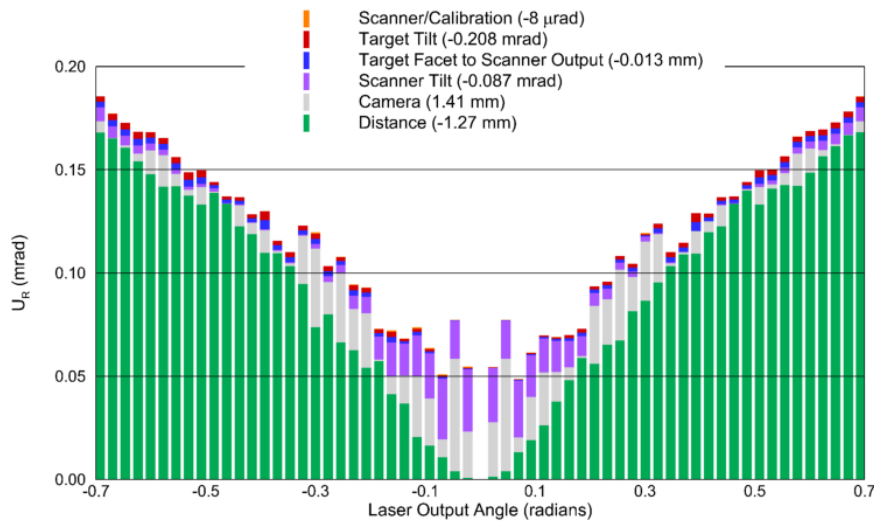


**Figure 28. Negative random error  $U_{R,i}^-$ . The contributing random errors to the negative random slope error uncertainty,  $U_{R,i}^-$ , were the tilt in the target, distance between the target face and scanner, scanner tilt, distance between the target face and collector vertex, camera calibration, and scanner/calibration.**

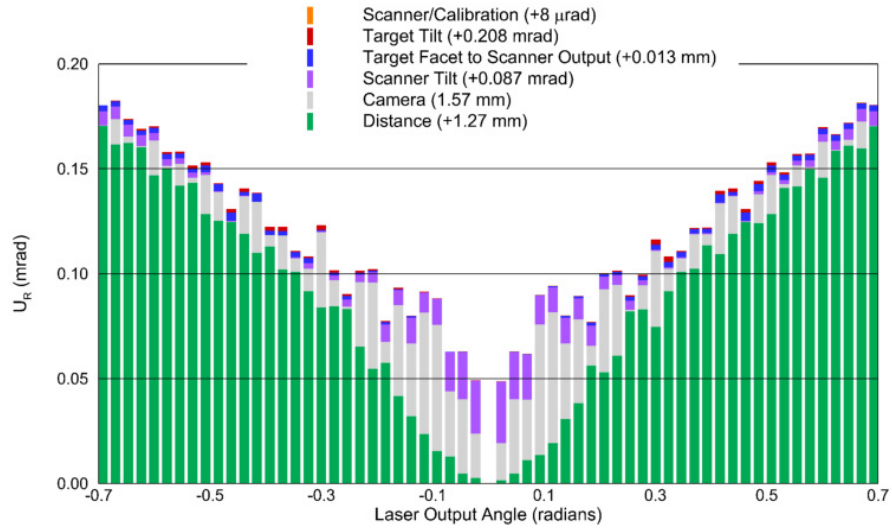


**Figure 29. Positive random error,  $U_{R+}$ . The contributing random errors to the positive random slope error uncertainty,  $U_{R,t+}$ , were the tilt in the target, distance between the target face and scanner, scanner tilt, distance between the target face and collector vertex, camera calibration, and scanner/calibration.**

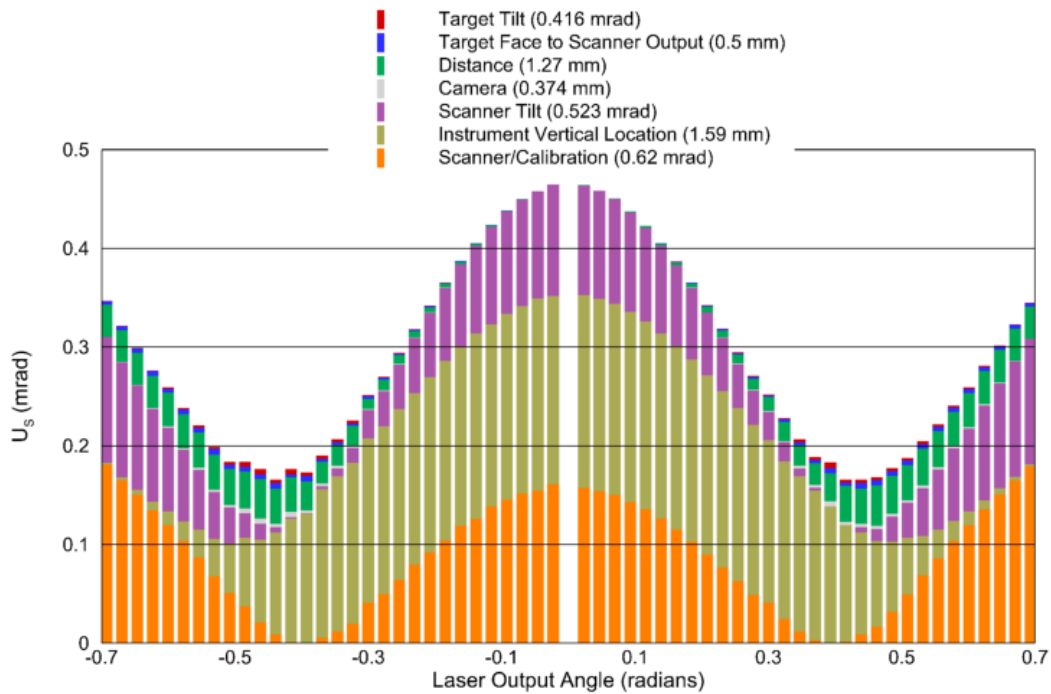
Seven systematic uncertainties were considered in this study ( $M=7$ ). These included measurement of the tilt in the target, distance between the target face and scanner, instrument vertical offset, scanner tilt, distance between the target face and collector vertex, camera calibration, and the scanner. The instrument vertical offset had the largest effect on the systematic uncertainty, with an average contribution of 42% or 0.12 mrad of error across the aperture (Table 6). The uncertainty in this measurement peaks at a laser output angle of zero radians, with a slope error of 0.19 mrad (Figure 30). The scanner calibration error was the second largest contributor to the systematic error, averaging 27% of the total error (Table 6). The uncertainty in the scanner calibration contributed up to 0.18 mrad of slope error. The laser output angle was the third largest contributor to the systematic uncertainty, averaging 19% of the total error (Table 6). This measurement’s average contribution to the slope error uncertainty was 0.06 mrad and peaked at 0.12 mrad (Figure 30).

To decrease the impact of the systematic uncertainty errors, the methods for determining the instrument vertical offset, scanner calibration process, and scanner tilt must be improved. Currently, the instrument vertical offset is measured using the human eye. If this measurement could be made with a mechanical device and the vertex could be accurately determined, the uncertainty would be greatly decreased. The scanner calibration is currently done by two operators—one controlling the scanner and the other checking the location of the laser on the scanner calibration grid. The likely cause for most of the error in this calibration is from the operator’s visual inspection of the laser location. If this process was automated, or if a camera were used to determine the laser location, the uncertainty in the scanner calibration would be reduced. To reduce the uncertainty in the laser output angle, the operator would need to level the laser to less than  $0.523$  mrad ( $0.03^\circ$ ) before each test. The inclinometers used to level the laser

have an accuracy of  $\pm 0.087$  mrad ( $0.005^\circ$ ). Improved inclinometer accuracy would reduce this uncertainty contribution.

**Table 6. Percentage contributions to the systematic slope error uncertainty.**

| Description                         | Average Contribution to the Uncertainty (%) | Maximum Contribution to the Uncertainty (%) | Minimum Contribution to the Uncertainty (%) |
|-------------------------------------|---------------------------------------------|---------------------------------------------|---------------------------------------------|
|                                     | $U_{S,i}$                                   | $U_{S,i}$                                   | $U_{S,i}$                                   |
| Target tilt                         | 0.8                                         | 3.2                                         | 0                                           |
| Target face to laser scanner output | 1.3                                         | 3.5                                         | 0                                           |
| Instrument vertical offset          | 42.3                                        | 81.5                                        | 0.6                                         |
| Scanner tilt                        | 19.1                                        | 36.9                                        | 0                                           |
| Distance from target to test piece  | 9.3                                         | 24.7                                        | 0                                           |
| Camera calibration                  | 0.2                                         | 0.7                                         | 0                                           |
| Scanner calibration                 | 27.0                                        | 52.1                                        | 0                                           |



: ] [ i fY' \$ "GngHYa U]Wg'cdY'YffcğzU<sub>s</sub>.

The systematic and random uncertainties must be combined to give the overall measurement uncertainty. There are over 30 degrees of freedom in this analysis, so the Root Sum Square,  $U_{RSS}$ , uncertainty model was used (Equation 13).  $U_R$ , and  $U_S$  were assumed to have a 95% confidence.

$$U_{RSS} = \pm [U_R^2 + U_S^2]^{\frac{1}{2}} \quad \text{Equation 13}$$

The positive and negative  $U_{RSS}$  uncertainty results are plotted in Figure 31.  $U_{RSS}^-$  has an average uncertainty of 0.32 mrad, with a maximum of 0.47 mrad and a minimum of 0.21 mrad.  $U_{RSS}^+$  has an average uncertainty of 0.32 mrad, with a maximum of 0.47 mrad and a minimum of 0.21 mrad. The RMS uncertainty was 0.33 mrad. The positive and negative results are essentially the same because the camera contribution (the only one with different positive and negative values) is relatively small. Thus for any given test we would expect that 95% of the time the RMS error would be less than 0.33 mrad.

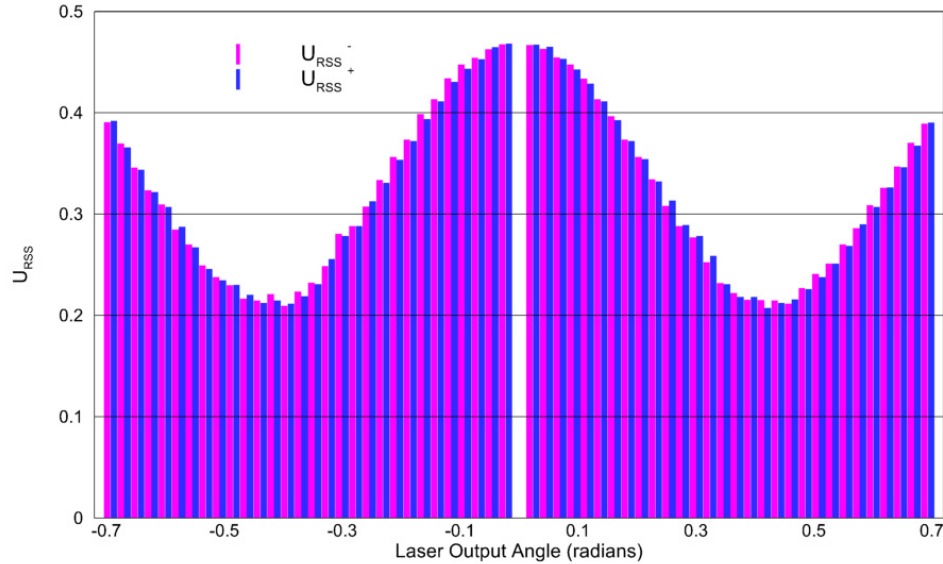


**Figure 31. Positive and negative  $U_{RSS}$  slope error uncertainty at the different laser output angles. The average uncertainty for  $U_{RSS}^-$  and  $U_{RSS}^+$  is 0.32 mrad.**

Each uncertainty contributes differently (i.e., randomly) to the total uncertainty over a set of tests. An error propagation analysis was completed to estimate the combined effect of these different uncertainties using the Monte Carlo method [1]. This was programmed in Excel to generate 20,000 trials where at each laser output angle a standard deviation was assigned according to the functional relationship for the average  $U_{RSS}$  shown in Fig. 31. A random slope error was then generated using the Box-Muller transformation [5] to achieve a normal (Gaussian) distribution. This is shown in Equation 14 below where  $a_1$  and  $a_2$  are random numbers between 0 and 1; then  $b$  is normally distributed with a mean of 0 and standard deviation of  $\sigma$ .

$$b = \sigma \sqrt{-2 \ln a_1} \cos(2\pi a_2) \quad \text{Equation 14}$$

As expected there are a small fraction of cases ( $\sim 5\%$ ) where the uncertainty is greater than  $2\sigma$ . The gap in the center at zero output angle represents the hole in the target where no return beams are captured. A distribution of these slope errors is shown in Fig. 32. The RMS of this distribution (with zero mean) is equivalent to the standard deviation, in this case 0.164 mrad.

Thus we would expect that 95% of the time, VSHOT test results for RMS error would be 0.33 mrad or less. The  $2\sigma$  slope error uncertainty will vary for a given test from about 0.21 to 0.46 mrad depending on the laser output angle and the resulting position along the aperture.

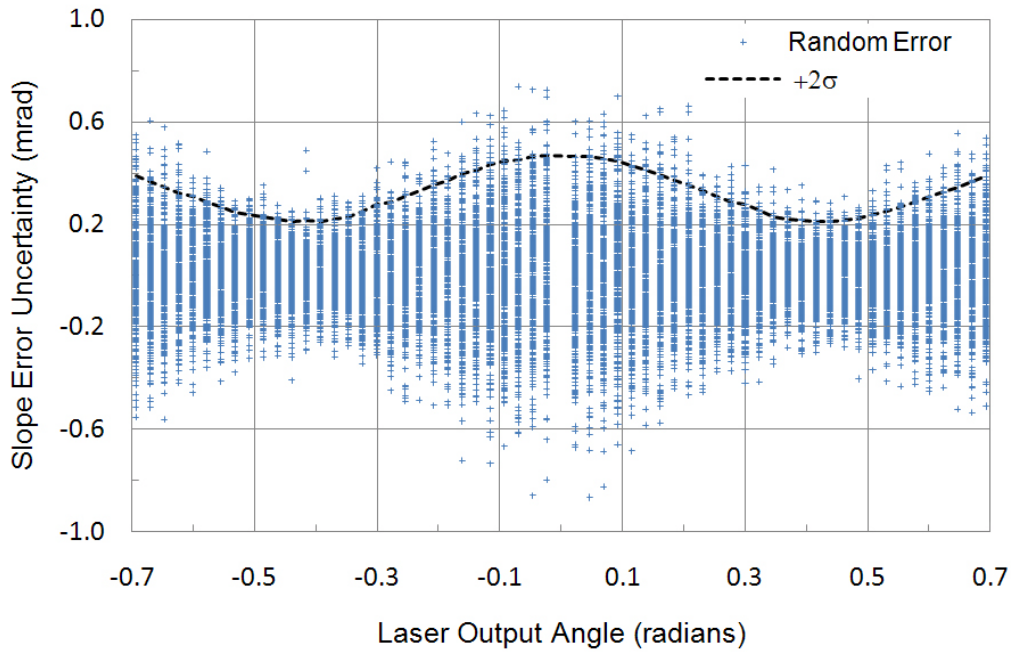


Figure 32. Slope error uncertainties at different laser output angles. The  $2\sigma$  uncertainty is shown for reference.

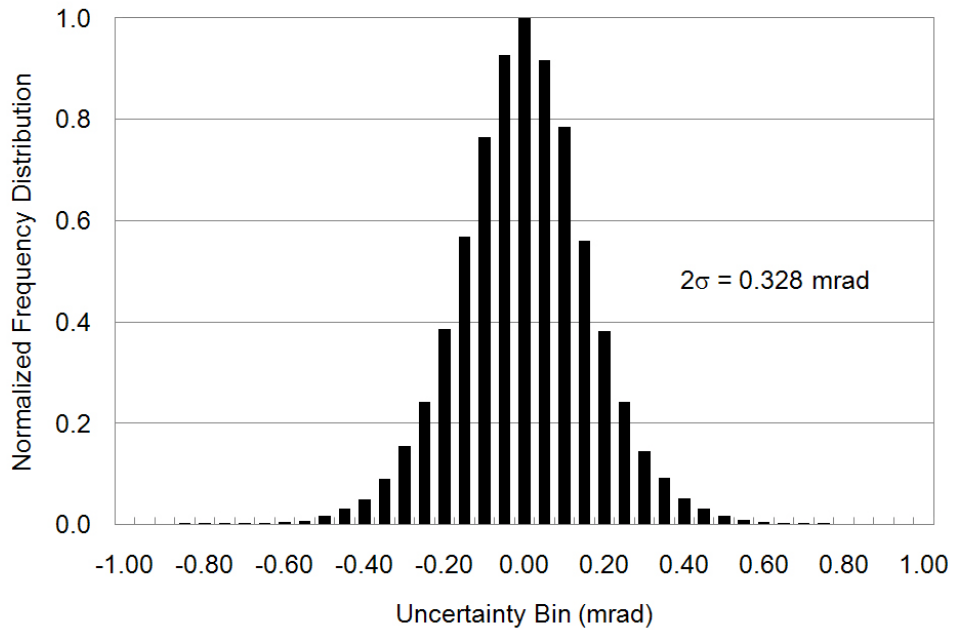


Figure 33. RMS slope error uncertainty for a VSHOT scan. This is a histogram of the RMS uncertainty for 20,000 tests.

## Uncertainty Estimate – Focal Length and Test Article Tilt

Each of the individual uncertainties and their contribution to estimated focal length and test article tilt were calculated to determine if these effects were significant. For each simulated scan across the aperture, the slope error versus y position was fit to the linear Zernike (Eq. 9) to yield the focal length and test article tilt. Only the random error in the distance measurement from the target to the test piece had any appreciable effect on the focal length,  $\pm 0.6$  mm. This is the only measurement that has a linear effect on the slope across a scan causing an error in the focal length term,  $B_2$ . All of the uncertainties have a relatively small effect on the calculated tilt term, ranging from 0.0007 mrad to 0.2 mrad as shown in Table 7. For field testing, a practically achievable tilt error of 1 mrad is considered low and all of the tilt terms listed in Table 7 are significantly lower. We did not consider the direct impact of test-article tilt error as a specific uncertainty error in this analysis because this value is one of the outputs of the data analysis. It is also very difficult to accurately determine this tilt in the field.

The same type error propagation analysis was used to estimate the combined effect of these different uncertainties on the focal length and tilt terms using the Monte Carlo method. A computer program similar to the one used to determine the slope error was written to calculate the effect on focal length and tilt. The program was run 20,000 times to determine the uncertainty in these terms with a 95% confidence ( $2\sigma$ ). The focal length uncertainty for VSHOT is  $\pm 0.6$  mm ( $2\sigma$ ), and the tilt uncertainty is  $\pm 0.2$  mrad ( $2\sigma$ ).

**Table 7. Uncertainty impacts on the focal length and test-article tilt.**

| Description                         | Focal Length Uncertainty |                      | Tilt Uncertainty                       |                          |
|-------------------------------------|--------------------------|----------------------|----------------------------------------|--------------------------|
|                                     | $U_{R,i}$                | $U_{S,i}$            | $U_{R,i}$                              | $U_{S,i}$                |
| Target tilt                         | negligible               | negligible           | $\pm 8 \mu\text{mrad}$                 | $\pm 0.02 \text{ mrad}$  |
| Target face to laser scanner output | negligible               | negligible           | $\pm 0.7 \mu\text{mrad}$               | $\pm 0.7 \mu\text{mrad}$ |
| Instrument vertical offset          |                          | negligible           |                                        | $\pm 0.2 \text{ mrad}$   |
| Laser output angle                  | negligible               | negligible           | $\pm 4 \mu\text{mrad}$                 | $\pm 0.03 \text{ mrad}$  |
| Distance from target to test piece  | $\pm 0.6 \text{ mm}$     | $\pm 0.2 \text{ mm}$ | negligible                             | negligible               |
| Camera calibration                  | negligible               | negligible           | $S_{\bar{R},i}^- = 0.5 \mu\text{mrad}$ | $0.7 \mu\text{mrad}$     |
| Scanner calibration                 | negligible               | negligible           | $S_{\bar{R},i}^+ = 0.7 \mu\text{mrad}$ | $\pm 0.03 \text{ mrad}$  |

## Summary

VSHOT has been used to characterize heliostat, dish, and trough reflector panels providing accurate surface slope information to determine the optical quality and to estimate optical performance. A 1997 uncertainty analysis showed that VSHOT had a RMS slope error uncertainty of about 0.1 mrad. The results in this analysis yield a higher  $2\sigma$  uncertainty,  $\sim 0.33$  mrad. The  $2\sigma$  uncertainty in the focal length is  $\pm 0.6$  mm (0.03%), and the tilt  $2\sigma$  uncertainty is  $\pm 0.2$  mrad. For a single test the expected  $2\sigma$  slope error will vary between 0.21 and 0.46 mrad depending on the laser output angle. The focal length uncertainty determined in the previous study was 0.8% and is slightly higher than this one. While there is no direct explanation for this there are many differences between these two studies. The original study was an experimental analysis that used a 16-inch-diameter telescope mirror and the current study is strictly analytical. The original study only used 0.0698 radian ( $4^\circ$ ) of the scanner cone angle and this one looks at the full 1.38 radians ( $80^\circ$ ). In addition, the original study did not attempt to separate the errors. The original study only looked at the RMS variation between tests, not the slope uncertainty at each output angle.

Out of the six random error sources considered, the measured distance between the target to test piece and camera calibration had the largest effects. The measured distance between the target face and collector vertex has the largest effect on the positive and negative random error,  $\sim 70\%$ , and the accuracy of this measurement is 1.27 mm. An accuracy of less than 1 mm would be needed to reduce the errors caused by this measurement. The camera was the second largest contributor on the positive and negative random uncertainty, contributing 14%–20% of the total error. A camera with more pixels would be needed to reduce this random error. This would increase the number of pixels per area and improve the software's ability to calculate the centroid of the return laser on the target, thus reducing the slope error uncertainty.

Seven systematic uncertainties were considered in this study. If the systematic uncertainty errors need to be decreased, the methods for determining the instrument vertical offset, scanner calibration process, and laser tilt will need to be improved. Currently, the instrument vertical offset is measured using the human eye and this has the largest effect on the systematic uncertainty, with an average contribution of 42%. The scanner/calibration error was the second-largest contributor to the systematic error, averaging 27% of the total error. The scanner calibration is currently done by two operators—one controlling the scanner and the other checking the location of the laser on the scanner calibration's grid. If this process was automated—or if a camera were used to determine the laser location—the uncertainty in the scanner calibration could be reduced. The laser output angle was the third-largest contributor to the systematic uncertainty, averaging 19% of the total error. To reduce the uncertainty in the laser output angle, the operator would need to level the laser to less than 0.523 mrad ( $0.03^\circ$ ) before each test.

The estimated uncertainty for slope error is relatively small compared to even the best parabolic trough mirror panel (2–3 mrad RMS slope error), and thus, there is currently little incentive to implement any of the improvements noted in this report. The estimated uncertainty in focal length and test-article tilt are extremely small compared to nominal values; thus, there is no

incentive to improve individual uncertainty contributions. Overall, it is safe to conclude that the uncertainty reported here is well within acceptable levels for the testing of parabolic troughs and very likely acceptable for dish or heliostat panels. Future work could extend this analysis to point-focus panels or to full panels where both x- and y-direction errors would be accounted for.

## Acknowledgements

This work was supported by the U.S. Department of Energy's Concentrating Power Program under Task Number CP09.1001.

## References

1. R. Dieck, *Measurement Uncertainty Methods and Applications, 4<sup>th</sup> Edition*. Research Triangle Park: The Instrumentation, Systems, and Automations Society, 2007.
2. S.A. Jones, J.K. Gruetzner, R.M. Houser, R.M. Edgar, and T.J. Wendelin, VSHOT Measurement Uncertainty and Experimental Sensitivity Study. *IECEC-97: Proceedings of the Thirty-Second Intersociety Energy Conversion Engineering Conference, 27 July–1 August 1997, Honolulu, Hawaii. Volume 3: Energy Systems, Renewable Energy Resources, Environmental Impact and Policy Impacts on Energy*, American Institute of Chemical Engineers, New York, NY, vol. 3, 1997, pp. 1877–1882.
3. J. Ojeda-Castaneda, *Optical Shop Testing, 2<sup>nd</sup> Edition*, edited by Malacara, 1992.
4. Model 6220H Galvanometer Optical Scanner Instruction Manual. Cambridge Technology, Inc., Revision 3.0, February 18, 2007.
5. G. Box and M. Muller "A Note on the Generation of Random Normal Deviates." *Ann. Math. Stat.* **29**, 610-611, 1958.



# REPORT DOCUMENTATION PAGE

*Form Approved*  
OMB No. 0704-0188

The public reporting burden for this collection of information is estimated to average 1 hour per response, including the time for reviewing instructions, searching existing data sources, gathering and maintaining the data needed, and completing and reviewing the collection of information. Send comments regarding this burden estimate or any other aspect of this collection of information, including suggestions for reducing the burden, to Department of Defense, Executive Services and Communications Directorate (0704-0188). Respondents should be aware that notwithstanding any other provision of law, no person shall be subject to any penalty for failing to comply with a collection of information if it does not display a currently valid OMB control number.

**PLEASE DO NOT RETURN YOUR FORM TO THE ABOVE ORGANIZATION.**

|                                                                                                                                                                                                                                                                                                                                                                                                                                                                                                                                                                                                                                                                                                                                                                                                                                                                                                                                                                                                                                                                                                                                                                                                                                                                                                                                                                                      |                                    |                                     |                                           |                            |                                                                       |                                     |  |  |
|--------------------------------------------------------------------------------------------------------------------------------------------------------------------------------------------------------------------------------------------------------------------------------------------------------------------------------------------------------------------------------------------------------------------------------------------------------------------------------------------------------------------------------------------------------------------------------------------------------------------------------------------------------------------------------------------------------------------------------------------------------------------------------------------------------------------------------------------------------------------------------------------------------------------------------------------------------------------------------------------------------------------------------------------------------------------------------------------------------------------------------------------------------------------------------------------------------------------------------------------------------------------------------------------------------------------------------------------------------------------------------------|------------------------------------|-------------------------------------|-------------------------------------------|----------------------------|-----------------------------------------------------------------------|-------------------------------------|--|--|
| <b>1. REPORT DATE (DD-MM-YYYY)</b><br>October 2010                                                                                                                                                                                                                                                                                                                                                                                                                                                                                                                                                                                                                                                                                                                                                                                                                                                                                                                                                                                                                                                                                                                                                                                                                                                                                                                                   |                                    |                                     | <b>2. REPORT TYPE</b><br>Milestone Report |                            |                                                                       | <b>3. DATES COVERED (From - To)</b> |  |  |
| <b>4. TITLE AND SUBTITLE</b><br>Visual Scanning Hartmann Optical Tester (VSHOT) Uncertainty Analysis                                                                                                                                                                                                                                                                                                                                                                                                                                                                                                                                                                                                                                                                                                                                                                                                                                                                                                                                                                                                                                                                                                                                                                                                                                                                                 |                                    |                                     |                                           |                            | <b>5a. CONTRACT NUMBER</b><br>DE-AC36-08-GO28308                      |                                     |  |  |
|                                                                                                                                                                                                                                                                                                                                                                                                                                                                                                                                                                                                                                                                                                                                                                                                                                                                                                                                                                                                                                                                                                                                                                                                                                                                                                                                                                                      |                                    |                                     |                                           |                            | <b>5b. GRANT NUMBER</b>                                               |                                     |  |  |
|                                                                                                                                                                                                                                                                                                                                                                                                                                                                                                                                                                                                                                                                                                                                                                                                                                                                                                                                                                                                                                                                                                                                                                                                                                                                                                                                                                                      |                                    |                                     |                                           |                            | <b>5c. PROGRAM ELEMENT NUMBER</b>                                     |                                     |  |  |
| <b>6. AUTHOR(S)</b><br>A. Gray, A. Lewandowski, and T. Wendelin                                                                                                                                                                                                                                                                                                                                                                                                                                                                                                                                                                                                                                                                                                                                                                                                                                                                                                                                                                                                                                                                                                                                                                                                                                                                                                                      |                                    |                                     |                                           |                            | <b>5d. PROJECT NUMBER</b><br>NREL/TP-5500-48482                       |                                     |  |  |
|                                                                                                                                                                                                                                                                                                                                                                                                                                                                                                                                                                                                                                                                                                                                                                                                                                                                                                                                                                                                                                                                                                                                                                                                                                                                                                                                                                                      |                                    |                                     |                                           |                            | <b>5e. TASK NUMBER</b><br>CP09.1001                                   |                                     |  |  |
|                                                                                                                                                                                                                                                                                                                                                                                                                                                                                                                                                                                                                                                                                                                                                                                                                                                                                                                                                                                                                                                                                                                                                                                                                                                                                                                                                                                      |                                    |                                     |                                           |                            | <b>5f. WORK UNIT NUMBER</b>                                           |                                     |  |  |
| <b>7. PERFORMING ORGANIZATION NAME(S) AND ADDRESS(ES)</b><br>National Renewable Energy Laboratory<br>1617 Cole Blvd.<br>Golden, CO 80401-3393                                                                                                                                                                                                                                                                                                                                                                                                                                                                                                                                                                                                                                                                                                                                                                                                                                                                                                                                                                                                                                                                                                                                                                                                                                        |                                    |                                     |                                           |                            | <b>8. PERFORMING ORGANIZATION REPORT NUMBER</b><br>NREL/TP-5500-48482 |                                     |  |  |
| <b>9. SPONSORING/MONITORING AGENCY NAME(S) AND ADDRESS(ES)</b>                                                                                                                                                                                                                                                                                                                                                                                                                                                                                                                                                                                                                                                                                                                                                                                                                                                                                                                                                                                                                                                                                                                                                                                                                                                                                                                       |                                    |                                     |                                           |                            | <b>10. SPONSOR/MONITOR'S ACRONYM(S)</b><br>NREL                       |                                     |  |  |
|                                                                                                                                                                                                                                                                                                                                                                                                                                                                                                                                                                                                                                                                                                                                                                                                                                                                                                                                                                                                                                                                                                                                                                                                                                                                                                                                                                                      |                                    |                                     |                                           |                            | <b>11. SPONSORING/MONITORING AGENCY REPORT NUMBER</b>                 |                                     |  |  |
| <b>12. DISTRIBUTION AVAILABILITY STATEMENT</b><br>National Technical Information Service<br>U.S. Department of Commerce<br>5285 Port Royal Road<br>Springfield, VA 22161                                                                                                                                                                                                                                                                                                                                                                                                                                                                                                                                                                                                                                                                                                                                                                                                                                                                                                                                                                                                                                                                                                                                                                                                             |                                    |                                     |                                           |                            |                                                                       |                                     |  |  |
| <b>13. SUPPLEMENTARY NOTES</b>                                                                                                                                                                                                                                                                                                                                                                                                                                                                                                                                                                                                                                                                                                                                                                                                                                                                                                                                                                                                                                                                                                                                                                                                                                                                                                                                                       |                                    |                                     |                                           |                            |                                                                       |                                     |  |  |
| <b>14. ABSTRACT (Maximum 200 Words)</b><br>In 1997, an uncertainty analysis was conducted of the Video Scanning Hartmann Optical Tester (VSHOT). In 2010, we have completed a new analysis, based primarily on the geometric optics of the system, and it shows sensitivities to various design and operational parameters. We discuss sources of error with measuring devices, instrument calibrations, and operator measurements for a parabolic trough mirror panel test. These help to guide the operator in proper setup, and help end-users to understand the data they are provided. We include both the systematic (bias) and random (precision) errors for VSHOT testing and their contributions to the uncertainty. The contributing factors we considered in this study are: target tilt; target face to laser output distance; instrument vertical offset; laser output angle; distance between the tool and the test piece; camera calibration; and laser scanner. These contributing factors were applied to the calculated slope error, focal length, and test article tilt that are generated by the VSHOT data processing. Results show the estimated 2-sigma uncertainty in slope error for a parabolic trough line scan test to be ±0.2 milliradians; uncertainty in the focal length is ±0.1 mm, and the uncertainty in test article tilt is ±0.04 milliradians. |                                    |                                     |                                           |                            |                                                                       |                                     |  |  |
| <b>15. SUBJECT TERMS</b><br>CSP; uncertainty analysis; VSHOT; parabolic trough; systematic error; random error; sensitivity                                                                                                                                                                                                                                                                                                                                                                                                                                                                                                                                                                                                                                                                                                                                                                                                                                                                                                                                                                                                                                                                                                                                                                                                                                                          |                                    |                                     |                                           |                            |                                                                       |                                     |  |  |
| <b>16. SECURITY CLASSIFICATION OF:</b>                                                                                                                                                                                                                                                                                                                                                                                                                                                                                                                                                                                                                                                                                                                                                                                                                                                                                                                                                                                                                                                                                                                                                                                                                                                                                                                                               |                                    |                                     | <b>17. LIMITATION OF ABSTRACT</b><br>UL   | <b>18. NUMBER OF PAGES</b> | <b>19a. NAME OF RESPONSIBLE PERSON</b>                                |                                     |  |  |
| <b>a. REPORT</b><br>Unclassified                                                                                                                                                                                                                                                                                                                                                                                                                                                                                                                                                                                                                                                                                                                                                                                                                                                                                                                                                                                                                                                                                                                                                                                                                                                                                                                                                     | <b>b. ABSTRACT</b><br>Unclassified | <b>c. THIS PAGE</b><br>Unclassified |                                           |                            | <b>19b. TELEPHONE NUMBER (Include area code)</b>                      |                                     |  |  |